

AN ASSESSMENT OF THE LONG-RANGE ELECTRIC  
QUADRUPOLE INTERACTIONS IN  
PRASEODYMIUM-FILLED SKUTTERUDITES

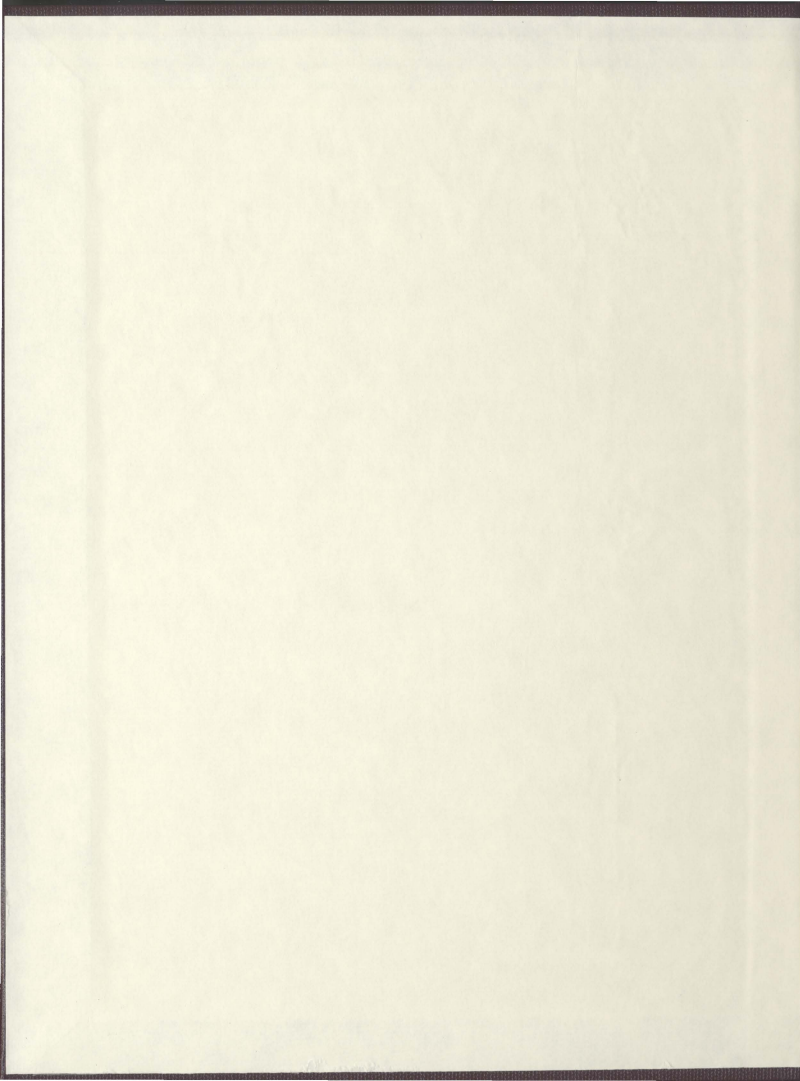
CENTRE FOR NEWFOUNDLAND STUDIES

---

**TOTAL OF 10 PAGES ONLY  
MAY BE XEROXED**

(Without Author's Permission)

RAM P. SAPKOTA







An assessment of the long-range electric quadrupole interactions in  
praseodymium-filled skutterudites

by

© Ram P. Sapkota  
M.Sc.(1996), B.Sc.(1993), Tribhuvan University of Nepal

A thesis submitted to the  
School of Graduate Studies  
in partial fulfillment of the  
requirements for the degree of  
Master of Science.

Department of Physics and Physical Oceanography  
Memorial University of Newfoundland

17 May 2005

ST. JOHN'S

NEWFOUNDLAND



Library and  
Archives Canada

Published Heritage  
Branch

395 Wellington Street  
Ottawa ON K1A 0N4  
Canada

Bibliothèque et  
Archives Canada

Direction du  
Patrimoine de l'édition

395, rue Wellington  
Ottawa ON K1A 0N4  
Canada

0-494-06657-1

*Your file* *Votre référence*

*ISBN:*

*Our file* *Notre référence*

*ISBN:*

#### NOTICE:

The author has granted a non-exclusive license allowing Library and Archives Canada to reproduce, publish, archive, preserve, conserve, communicate to the public by telecommunication or on the Internet, loan, distribute and sell these worldwide, for commercial or non-commercial purposes, in microform, paper, electronic and/or any other formats.

The author retains copyright ownership and moral rights in this thesis. Neither the thesis nor substantial extracts from it may be printed or otherwise reproduced without the author's permission.

#### AVIS:

L'auteur a accordé une licence non exclusive permettant à la Bibliothèque et Archives Canada de reproduire, publier, archiver, sauvegarder, conserver, transmettre au public par télécommunication ou par l'Internet, prêter, distribuer et vendre des thèses partout dans le monde, à des fins commerciales ou autres, sur support microforme, papier, électronique et/ou autres formats.

L'auteur conserve la propriété du droit d'auteur et des droits moraux qui protègent cette thèse. Ni la thèse ni des extraits substantiels de celle-ci ne doivent être imprimés ou autrement reproduits sans son autorisation.

---

In compliance with the Canadian Privacy Act some supporting forms may have been removed from this thesis.

Conformément à la loi canadienne sur la protection de la vie privée, quelques formulaires secondaires ont été enlevés de cette thèse.

While these forms may be included in the document page count, their removal does not represent any loss of content from the thesis.

Bien que ces formulaires aient inclus dans la pagination, il n'y aura aucun contenu manquant.

  
**Canada**

# Abstract

Praseodymium-filled skutterudites  $RT_4X_{12}$  are body centered cubic (bcc) structures that belong to the space group  $Im\bar{3}$  (no.204) where R stands for rare earth elements (Pr, Ce, La, U, etc.), T stands for transition metal ions (Fe, Ru, Os) and X represents pnictogens (P, As, Sb). Three different praseodymium-filled skutterudites are considered in the present study:  $PrFe_4P_{12}$ ,  $PrOs_4Sb_{12}$  and  $PrRu_4P_{12}$ . These materials were explored for their crystal structure and interesting properties. Calculations are made of the following: i) the electric quadrupole moment possessed by the Pr  $4f^2$  ground state doublet, ii) the electric quadrupole moment produced by unique displacements of transition metal ions, creating a cubic to tetragonal type of distortion in the crystal, and iii) long-range quadrupole interactions between the Pr  $4f^2$  electrons and the transition metal ions. Neglecting the screening effect of the conduction electrons, the quadrupole moment associated with the ground state of the Pr  $4f^2$  electrons and with the transition metal ions are found to have similar values when a crude approximation to the radial part of  $4f^2$  electrons is used. Long-range quadrupole interactions between the Pr  $4f^2$  electrons and the transition metal ions are calculated for their three different alignments. The attractive and repulsive quadrupole interactions exhibited by the two linear quadrupoles based on their different alignments are discussed in the present work. This is a first step for creating a dynamical theory of electric quadrupole interactions in praseodymium-filled skutterudites. A complete dynamical

theory should include contributions from long- and short-range quadrupole interactions among the conduction electrons, the Pr  $4f^2$  electrons, and the transition metal ions. The present work is limited to the long-range quadrupole interactions between the Pr  $4f^2$  electrons and the transition metal ions. Further studies focusing on long- and short-range electric quadrupole interactions among the conduction electrons, the Pr  $4f^2$  electrons and the transition metal ions would be essential in order to more fully develop the desired theory.

## Acknowledgements

The author would like to thank Dr. S. H. Curnoe for supervising the present work, and Dr. J. Lagowski for providing me with her computer for research. I wish to thank Mr. Lester Marshall of the University Counselling Centre for proofreading this thesis. Last but not least, thanks to my wife, Mina, and son, Aayush, for their patience and great support during my long hours in research.



# Contents

Abstract	ii
Acknowledgements	iv
Table of Contents	vii
List of Tables	viii
List of Figures	ix
<b>1 Introduction</b>	<b>1</b>
1.1 Overview . . . . .	1
1.2 Crystal structure of skutterudites . . . . .	2
1.3 Properties of praseodymium-filled skutterudites . . . . .	2
1.3.1 $\text{PrFe}_4\text{P}_{12}$ . . . . .	4
1.3.2 $\text{PrRu}_4\text{P}_{12}$ . . . . .	4
1.3.3 $\text{PrOs}_4\text{Sb}_{12}$ . . . . .	5
1.4 Hund's rules . . . . .	5
1.5 Crystal field splitting . . . . .	6
1.6 The Wigner-Eckart theorem . . . . .	8
1.7 Multipole expansion of the potential of a localized charge distribution	9

1.8	Properties of a linear quadrupole . . . . .	11
1.9	Electrostatic energy of a localized charge distribution in an external field	12
1.10	The long-range quadrupole-quadrupole interaction energy $U_{quad}$ formulation . . . . .	13
1.11	Quadrupole-quadrupole interaction energy $U_{quad}$ for the three different alignments of linear quadrupoles . . . . .	15
1.11.1	Case I: Two quadrupoles aligned along the $z$ -axis . . . . .	15
1.11.2	Case II: Two quadrupoles along the $x$ - and $z$ -axes . . . . .	16
1.11.3	Case III: Two quadrupoles along the $y$ - and $z$ -axes . . . . .	17
1.12	Organization of the present work . . . . .	19
<b>2</b>	<b>Quadrupole Interactions in Filled Skutterudites</b>	<b>20</b>
2.1	Quadrupole moment calculation by using the Wigner-Eckart theorem	20
2.2	Approximation of the radial part $\mathcal{A}$ of the $f$ -electron wave function . .	22
2.3	The Clebsch-Gordan decomposition of $J = 4$ Pr $4f^2$ electrons into $l_1 = 3$ , $l_2 = 3$ and $S = 1$ . . . . .	23
2.4	Angular charge density formulation . . . . .	25
2.4.1	Wave function for one spin $1/2$ particle . . . . .	25
2.4.2	Wave function for two spin-less particles . . . . .	26
2.4.3	Wave function for two particles with spin . . . . .	28
2.5	Quadrupole moment possessed by the Pr $4f^2$ electrons in $ \Gamma_3^- \rangle$ and $ \Gamma_3^+ \rangle$ states . . . . .	29
2.6	Quadrupole moment due to the displacement of T metal ions . . . . .	36
2.7	The long-range quadrupole-quadrupole interaction energies $U_{quad}$ between the Pr $4f^2$ electrons and T metal ions . . . . .	39
2.8	Interpretation . . . . .	40

<b>3 Discussion and Summary</b>	<b>44</b>
3.1 Discussion . . . . .	44
3.2 Summary . . . . .	47
<b>A Appendix</b>	<b>49</b>
A.1 Electric field gradient due to a quadrupole . . . . .	49
A.2 Spherical Harmonics . . . . .	50
<b>Bibliography</b>	

## List of Tables

2.1	The lattice constants and quadrupole moments possessed by the T metal ions due to $(\beta, \beta, -2\beta)$ displacement from their initial positions where $\beta \approx 10^{-4}a$ . . . . .	39
2.2	The long-range Pr-Pr quadrupole interaction energies between the Pr $4f^2$ electrons in states $ \Gamma_3^+\rangle$ and $ \Gamma_3^-\rangle$ where $\mathcal{A}$ has units of $m^2$ . . . . .	40
2.3	The long-range T-T (Fe-Fe, Os-Os, Ru-Ru) quadrupole interaction energies between the T metal ions displaced in directions $(\beta, \beta, -2\beta)$ and $(-\beta, -\beta, 2\beta)$ where $\beta$ has units of m. . . . .	41
2.4	The long-range Pr-T (Pr-Fe, Pr-Os, Pr-Ru) quadrupole interaction energies between the Pr $4f^2$ electrons in state $ \Gamma_3^\mp\rangle$ and T metal ions displaced in the directions $(\pm\beta, \pm\beta, \mp 2\beta)$ where $\mathcal{A}$ has the units of $m^2$ and $\beta$ has units of m. . . . .	41
2.5	Comparison of quadrupole-quadrupole interaction energies in $\text{PrFe}_4\text{P}_{12}$ for $N = 1$ . . . . .	42
2.6	Comparison of quadrupole-quadrupole interaction energies in $\text{PrFe}_4\text{P}_{12}$ for $N = 2$ . . . . .	42

# List of Figures

1.1	A bcc unit cell of praseodymium-filled skutterudite . . . . .	3
1.2	Spin occupation of the $4f^2$ electrons to seven degenerate orbitals according to Hund's rules. . . . .	6
1.3	A general charge distribution enclosed in a given volume. . . . .	10
1.4	A linear quadrupole with charges $q, -2q$ and $q$ aligned along the $y$ -axis where $b$ is the distance between opposite charges. . . . .	11
1.5	Case I: Two quadrupoles aligned along the $z$ -axis. . . . .	16
1.6	Case II : Two quadrupoles along the $x$ - and $z$ -axes. . . . .	17
1.7	Case III : Two quadrupoles aligned along the $y$ - and $z$ -axes. . . . .	18

# Chapter 1

## Introduction

### 1.1 Overview

Praseodymium-filled skutterudites  $RT_4X_{12}$  (R stands for rare earth ions (La, Ce, Pr, etc.), T denotes the transition metal ions (Fe, Os, Ru) and X stands for pnictogens (P, As, Sb) are materials of current scientific interest because they exhibit various interesting properties at low temperatures: heavy fermion behavior, structural phase transitions due to electron correlations, unconventional superconductivity, and thermoelectric property for industrial applications [1–3]. In order to assess the long-range quadrupole-quadrupole interactions in praseodymium-filled skutterudites, the following are considered for the present study:  $PrFe_4P_{12}$ ,  $PrOs_4Sb_{12}$ , and  $PrRu_4P_{12}$ .

$PrFe_4P_{12}$  undergoes a partial metal-insulator transition accompanied by anti-quadrupolar ordering at  $T = 6.7\text{K}$  [1, 3, 4].  $PrRu_4P_{12}$  shows a metal-insulator transition at  $\sim 60\text{K}$  followed by an unidentified ordering at  $\sim 2\text{K}$  [4–6].  $PrOs_4Sb_{12}$  exhibits heavy fermion superconductivity below  $1.85\text{K}$  [1, 2]. Quadrupole interactions are implicated in all of these materials.

So far, little effort has been made to develop a theory of quadrupole interactions

in the filled skutterudites considered in this thesis. An in-depth study is required of the long- and short-range quadrupole-quadrupole interactions among the conduction electrons, the transition metal ion (T) displacements and the Pr  $4f^2$  electrons to fully develop a complete theory for these interactions. The present study on long-range quadrupole-quadrupole interactions between the Pr  $4f^2$  electrons and the transition metal ion displacements is a first step toward developing a theory of quadrupole interactions in the praseodymium-filled skutterudites. Although the displacement of pnictogen ions may also possess a quadrupole moment [4, 7], these will not be considered in the present work; however the results for the transition metal ions could easily be extended to the pnictogens.

## 1.2 Crystal structure of skutterudites

Numerous authors have studied the crystal structure of filled skutterudites [8–13]. Fig. 1.1 shows a body-centered cubic (bcc) unit cell of a filled skutterudite  $RT_4X_{12}$  (e.g.,  $PrFe_4P_{12}$ ). Each bcc unit cell is composed of 34 ions: 2R, 8T and 24X ions [14] where each T ion is surrounded by six pnictogens, and each R ion is surrounded by eight T ions. In each bcc unit cell, an R ion takes its position at the origin and at the corners, and each of the T ions are positioned midway between the R ions. If  $a$  is the lattice constant of the bcc cell, the positions of the two R ions and a T ion in the cell are  $(0, 0, 0)$ ,  $(\frac{a}{2}, \frac{a}{2}, \frac{a}{2})$  and  $(\frac{a}{4}, \frac{a}{4}, \frac{a}{4})$ , respectively.

## 1.3 Properties of praseodymium-filled skutterudites

This section discusses the properties of the praseodymium-filled skutterudites considered in this thesis. The Pr ions of the filled skutterudites are trivalent [3, 15],

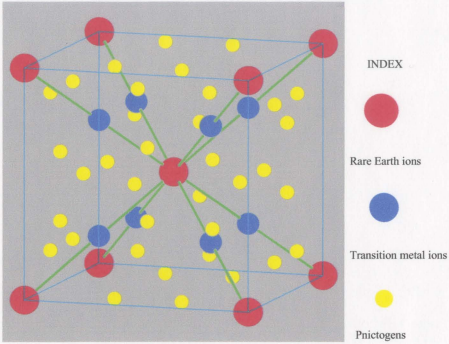


Figure 1.1: A bcc unit cell of praseodymium-filled skutterudite

therefore there are 2 f-electrons. They have total angular momentum  $J = 4$ , as determined by Hund's rules (see Section 1.4). These nine-fold degenerate states split into a singlet ( $\Gamma_1$ ), a doublet ( $\Gamma_3$ ), and two triplets ( $\Gamma_4$ ) and ( $\Gamma_5$ ) under crystal field splitting [6, 16] (see Section 1.5).

Grandjean et al. have inferred an oxidation state of 2+ for Fe in  $RFe_4P_{12}$  ( $R = \text{Ce or Pr}$ ) based on X-ray diffraction measurements which suggest P-P bonding [17]. It is reasonable to assume an oxidation number 2+ for Ru and Os ions since these ions have the same valence electron counts as Fe. In all filled skutterudites, the iron is non-magnetic [12, 13, 17].

There is still some controversy about the crystal field ground state of the Pr  $4f^2$  electrons [1, 2, 18–20]. Experiments have shown that in all three compounds ( $\text{PrFe}_4\text{P}_{12}$ ,  $\text{PrOs}_4\text{Sb}_{12}$ , and  $\text{PrRu}_4\text{P}_{12}$ ) the ground state is non-magnetic, therefore it must be either the singlet or the doublet, since both the triplets are magnetic. We



consider the  $\Gamma_3$  doublet to be the ground state in this thesis; however the analysis we present may be extended to the case when the  $\Gamma_1$  singlet is the ground state with a low-lying magnetic triplet excited state [21, 22]. In this case, the quadrupole moment carried by the triplet is responsible for the quadrupole interactions.

### 1.3.1 $\text{PrFe}_4\text{P}_{12}$

$\text{PrFe}_4\text{P}_{12}$  shows a partial metal to insulator transition, seen as a sharp upturn of the resistivity, at  $T = 6.7\text{K}$ . This is accompanied by anti-quadrupolar ordering, observed directly in in-field neutron diffraction measurements [23], and a structural phase transition involving the Fe ions displacement [24]. In both  $\text{PrFe}_4\text{P}_{12}$  and  $\text{PrRu}_4\text{P}_{12}$  (discussed below), the structural phase transition doubles the unit cell and opens a gap at the Fermi surface. Unlike the case of  $\text{PrRu}_4\text{P}_{12}$ , at very low temperatures, the resistivity tends to zero due to the presence of carriers on an additional Fermi surface.

At high magnetic fields a heavy electron state is observed with effective mass larger than  $60m_e$  [1, 3, 18, 25–30] where  $m_e$  is the mass of an electron  $\sim 9.1 \times 10^{-31}\text{kg}$ . This phenomenon has not been linked to quadrupolar interactions, therefore, is not directly related to the subject of this thesis.

### 1.3.2 $\text{PrRu}_4\text{P}_{12}$

$\text{PrRu}_4\text{P}_{12}$  undergoes M-I transition at  $T_{M-I} = 60\text{K}$  accompanied by a structural phase transition, but there is no magnetic or quadrupolar ordering associated with this transition [6]. Both Ru and P ion displacements have been implicated in this transition [4, 7]. Some kind of non-magnetic ordering is observed at very low temperatures,  $T \approx 1\text{K}$ , which has been conjectured to be quadrupolar [4, 31].

### 1.3.3 $\text{PrOs}_4\text{Sb}_{12}$

$\text{PrOs}_4\text{Sb}_{12}$  exhibits heavy fermion superconductivity below  $T_c = 1.85\text{K}$  [1, 2, 32]. It is the first Pr-based heavy fermion superconductor and the first among the family of filled skutterudite compounds. It has been speculated that superconductivity is mediated by quadrupolar interactions [2]; if so, then it represents a new mechanism for superconductivity distinct from phonons or spin fluctuations. Nodes in the gap function indicate that superconductivity is unconventional, but the exact symmetry of the order parameter is still undetermined [33].

The heavy fermion behavior in  $\text{PrOs}_4\text{Sb}_{12}$  may be due to the interactions between the electric quadrupole moment associated with non-spherical charge distribution of the Pr  $4f^2$  electrons and the electric quadrupole moment of the conduction electrons. This was formulated as the two-channel Kondo model by D. L. Cox [34]. In contrast, in case of Ce- and U-based compounds, heavy fermion behavior is due to the interaction between the magnetic dipole moments of the Ce- and U-ions, and the spins of the conduction electrons [1, 2].

## 1.4 Hund's rules

Hund's rules are useful in determining the ground state of the Pr  $4f^2$  electrons. Numerous texts are available to study Hund's rules [35–38]. Hund's rules state that the eigenvalue of the total angular momentum is  $J = |L - S|$  if the shell is less than half-filled, and  $L + S$  if the shell is more than half filled. This rule is called spin-orbit coupling or  $LS$  coupling, and it applies to the present study in determining the ground state of the Pr  $4f^2$  electrons.

Hund's rules can also be stated as follows: when an atom has orbitals of equal en-

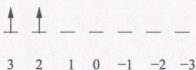


Figure 1.2: Spin occupation of the  $4f^2$  electrons to seven degenerate orbitals according to Hund's rules.

ergy, the order in which they are filled by electrons is such that a maximum number of electrons have parallel spins. The angular momentum quantum number for the ground state configuration of the Pr  $4f^2$  electrons can be calculated using this rule. The possible magnetic quantum numbers associated with  $l = 3$  are:  $m_l = 3, 2, 1, 0, -1, -2, -3$ . Parallel spins fill these states in this order. When there are more than seven electrons, the opposite spin states begin to fill. The total orbital and spin angular momenta associated with the Pr  $4f^2$  electrons are therefore  $L = 5$  and  $S = 1$ . Since the shell is less than half filled in case of the Pr  $4f^2$  electrons,  $J = L - S = 4$ .

For very heavy atoms (such as Pb, Bi, Po, etc.), we first calculate the total angular momentum from each electron, then add up the  $J$ 's. This is called  $jj$  coupling where  $j$  is an eigenvalue of  $J$ . As  $\text{Pr}^{3+}$  is not a heavy metal,  $jj$  coupling does not apply to the present study.

## 1.5 Crystal field splitting

The crystal field of the eight transition metal ions which surround each  $\text{Pr}^{3+}$  ion lifts the nine-fold degeneracy of the  $J = 4$  Pr  $4f^2$  electrons into a singlet ( $\Gamma_1$ ), two triplets ( $\Gamma_4$  and  $\Gamma_5$ ) and a doublet ( $\Gamma_3^\pm$ ) [18]. This phenomenon is called crystal field splitting. All the split states can be expressed in terms of  $|j, m_j\rangle$  for  $J = 4$  and

$m_j = 4, 3, 2, 1, 0, -1, -2, -3, -4$  which are as follows [21, 39]:

$$\begin{aligned}
 |\Gamma_1\rangle &= \sqrt{\frac{5}{24}} (|4, 4\rangle + |4, -4\rangle) + \sqrt{\frac{7}{12}} |4, 0\rangle \\
 |\Gamma_3^+\rangle &= \sqrt{\frac{7}{24}} (|4, -4\rangle + |4, 4\rangle) - \sqrt{\frac{5}{12}} |4, 0\rangle \\
 |\Gamma_3^-\rangle &= \sqrt{\frac{1}{2}} (|4, -2\rangle + |4, 2\rangle) \\
 |\Gamma_4^0\rangle &= \sqrt{\frac{1}{2}} (|4, 4\rangle - |4, -4\rangle) \\
 |\Gamma_4^\pm\rangle &= \sqrt{\frac{1}{8}} |4, \pm 3\rangle + \sqrt{\frac{7}{8}} |4, \mp 1\rangle \\
 |\Gamma_5^0\rangle &= \sqrt{\frac{1}{2}} (|4, 2\rangle - |4, -2\rangle) \\
 |\Gamma_5^\pm\rangle &= \sqrt{\frac{7}{8}} |4, \pm 3\rangle - \sqrt{\frac{1}{8}} |4, \mp 1\rangle.
 \end{aligned} \tag{1.1}$$

A single f-electron ( $L = 3, S = \frac{1}{2}$ ) has 14 degenerate states. For two f-electrons, the total possible number of degenerate states is  $14^2 = 196$  which are subject to the Pauli exclusion principle (anti-symmetrization).  $14 \times \frac{15}{2} = 105$  of these states are specified by symmetric wave functions and remaining  $14 \times \frac{13}{2} = 91$  states by antisymmetric wave functions. The degenerate states defined by the antisymmetric wave functions are of interest in the present study as they are the degenerate states pertinent to the Pr  $4f^2$  electrons.

The Hund's rules select the nine degenerate states i.e.,  $J = 4$  out of these 91 states, where these nine-fold degenerate states should be the linear combinations of the basis functions [40]:

$$\begin{aligned}
 |4, m_j\rangle &= \sum_{(m_{l_1}, m_{l_2}, m_{s_1}, m_{s_2}, m_j)} \alpha(m_{l_1}, m_{l_2}, m_{s_1}, m_{s_2}, m_j) |3, m_{l_1}\rangle \otimes |1/2, m_{s_1}\rangle \\
 &\quad \otimes |3, m_{l_2}\rangle \otimes |1/2, m_{s_2}\rangle,
 \end{aligned} \tag{1.2}$$

where  $m_{l_1}$  and  $m_{l_2}$  are the possible eigenvalues of the orbital angular momentum  $L_{1z}$  and  $L_{2z}$  for the Pr  $4f^2$  electrons and  $m_{s_1}$  and  $m_{s_2}$  are the possible eigenvalues of

spin angular momentum  $S_{1z}$  and  $S_{2z}$  of these electrons.  $\alpha(m_{l_1}, m_{l_2}, m_{s_1}, m_{s_2}, m_j)$  are Clebsch-Gordan coefficients which will be dealt in Section 2.3.

## 1.6 The Wigner-Eckart theorem

The Wigner-Eckart theorem relates matrix elements of vector operators to matrix elements of the total angular momentum operator  $\vec{J}$ . By using the total angular momentum,  $J = 4$ , for the Pr  $4f^2$  electrons, the quadrupole moment associated with it can be calculated using the Wigner-Eckart theorem.

An observable  $\vec{V}$  is a vector operator if its components  $V_x$ ,  $V_y$  and  $V_z$  satisfy the following commutation relations with the components of angular momentum operator  $\vec{J}$ :

$$[J_i, V_j] = i\hbar\epsilon_{ijk}V_k, \quad (1.3)$$

where  $\epsilon_{ijk}$  is the Levi-Civita antisymmetric tensor and  $\hbar$  is Planck's constant. Note that:

$$[J_i, J_j] = i\hbar\epsilon_{ijk}J_k, \quad (1.4)$$

is a special case of Eq. 1.3.

The Wigner-Eckart theorem states that the matrix elements of any vector operator in a sub-space spanned by  $|JM\rangle$  for fixed  $J$  and  $M = \pm J, \pm(J-1), \dots$ , are proportional to the matrix elements of the angular momentum operator  $\vec{J}$  [41]. Mathematically:

$$\langle JM | \vec{V} | J' M' \rangle = \alpha(k, J) \langle JM | \vec{J} | J' M' \rangle, \quad (1.5)$$

where  $\alpha(k, J)$  is the proportionality constant, and  $k$  is an eigenvalue associated with a different operator than  $J^2$  or  $J_z$ . The Wigner-Eckart theorem also applies to tensors [42-44]. The  $Q_{33}$  component of the quadrupole moment can be calculated as :

$$Q_{33} = e \int (3z^2 - r^2)\rho(\vec{r})d^3r, \quad (1.6)$$

where  $\rho(\vec{r})$  is the number density of charges, and  $e$  is the charge of a positron,  $1.60217733 \times 10^{-19}\text{C}$ . A general formula for the quadrupole moment will be derived and discussed in detail in Chapter 2. The matrix elements of the Cartesian quadrupole moment operator,  $(3z^2 - r^2)$ , are proportional to the matrix elements of the operator  $(3J_z^2 - J^2)$ :

$$\langle JM | 3z^2 - r^2 | JM \rangle = \alpha(k, J) \langle JM | (3J_z^2 - J^2) | JM \rangle. \quad (1.7)$$

We will make use of this in Section 2.3.

## 1.7 Multipole expansion of the potential of a localized charge distribution

The potential at a far point P is the same as if there were, at the origin, a monopole, plus a dipole, plus a quadrupole, etc., where  $r$  is larger than the maximum value of  $r'$ . Fig. 1.3 shows a charge distribution confined in a given volume near the origin. The potential at a distance  $r \gg r'$  due to the charge density,  $\rho(\vec{r}')$ , is determined by using the Taylor expansion of  $1/|\vec{r} - \vec{r}'|$  about  $\vec{r}' = 0$ . The multipole expansion of the potential of a charge distribution is discussed in a number of texts [42–48].

The potential at a distance  $r$  from the origin is:

$$\Phi(\vec{r}) = \frac{1}{4\pi\epsilon_0} \int \frac{\rho(\vec{r}') d^3r'}{|\vec{r} - \vec{r}'|}, \quad (1.8)$$

where  $\epsilon_0$  is the permittivity of the free space. Note that SI units are used throughout the thesis. The multipole expansion of the potential about the origin is:

$$\Phi(\vec{r}) = \frac{1}{4\pi\epsilon_0} \left[ \frac{q}{r} + \frac{\vec{P} \cdot \vec{r}}{r^3} + \frac{r_i Q_{ij} r_j}{2r^5} + \dots \right], \quad (1.9)$$

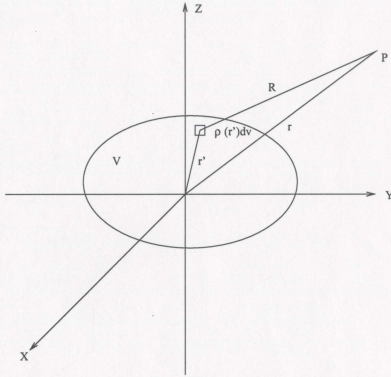


Figure 1.3: A general charge distribution enclosed in a given volume.

where  $q = \int \rho(\vec{r}') d^3r'$  is the expression for the total charge,  $\vec{P} = \int \vec{r}' \rho(\vec{r}') d^3r'$  is the expression for dipole moment, and the quadrupole moment  $Q_{ij}$  can be expressed as:

$$Q_{ij} = \int (3r_i r_j - r^2 \delta_{ij}) \rho(\vec{r}') d^3r'. \quad (1.10)$$

The convention that repeated indices are summed is used throughout the thesis. From the definition 1.10,  $Q_{ij}$  is traceless and symmetric. Although there are five independent components of  $Q_{ij}$ , of which 3 usually specify an orientation and 2 specify intensities, only one of them becomes a characteristic quadrupole moment whenever an axially symmetric charge distribution is considered. For instance,  $Q_{33}$  becomes a characteristic quadrupole moment for a charge distribution symmetric to the  $z$ -axis.

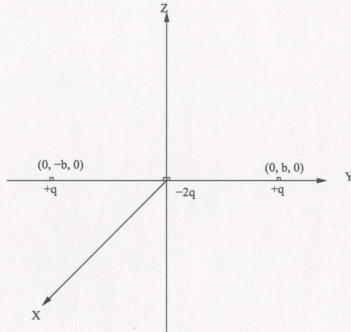


Figure 1.4: A linear quadrupole with charges  $q, -2q$  and  $q$  aligned along the  $y$ -axis where  $b$  is the distance between opposite charges.

## 1.8 Properties of a linear quadrupole

A number of texts have described the formulation of quadrupole moments via multipole expansion of a continuous (or discrete) charge distribution [43, 44, 47]. A linear quadrupole with a charge distribution that is symmetric about the  $y$ -axis is shown in Fig. 1.4. The charges  $q, -2q$  and  $q$  are located at the points  $(0, -b, 0)$ ,  $(0, 0, 0)$  and  $(0, b, 0)$  respectively, where  $b$  is the distance between positive and negative charges. The charge density of a point charge  $q$ , located at point  $(x', y', z')$  is:

$$\rho(\vec{r}) = q\delta(x - x')\delta(y - y')\delta(z - z'), \quad (1.11)$$

where  $\delta$  is Dirac delta function. The charge density of the linear quadrupole shown in Fig. 1.4 is calculated by using Eq. 1.11:

$$\rho(\vec{r}) = q\delta(x)\delta(y - b)\delta(z) - 2q\delta(x)\delta(y)\delta(z) + q\delta(x)\delta(y + b)\delta(z). \quad (1.12)$$



From Eqs. 1.10 and 1.12, the calculation of  $Q_{ij}$  for the linear quadrupole in Fig. 1.4 is straightforward:

$$Q_{ij} = \int (3r_i r_j - r^2 \delta_{ij}) \left( q\delta(x)\delta(y-b)\delta(z) - 2q\delta(x)\delta(y)\delta(z) + q\delta(x)\delta(y+b)\delta(z) \right) d^3r, \quad (1.13)$$

where  $d^3r = dx dy dz$  is used for the Cartesian system of co-ordinates.

The quadrupole moment along the  $y$ -axis,  $Q_{22} = 4qb^2$  is the characteristic quadrupole moment for the quadrupole in Fig. 1.4. The quadrupole moment along the  $x$ -axis  $Q_{11}$  and along the  $z$ -axis  $Q_{33}$  can be expressed in terms of the characteristic quadrupole moment  $Q_{22}$  as:  $Q_{11} = Q_{33} = -\frac{1}{2}Q_{22} = -2qb^2$ . All of the off-diagonal components are zero, i.e.,  $Q_{12} = Q_{13} = Q_{23} = 0$ .

## 1.9 Electrostatic energy of a localized charge distribution in an external field

This section deals with the multipole expansion of the electrostatic energy of a charge distribution under the influence of an external field. The electrostatic interaction energy of a charge distribution in an external field is the sum of the interactions of the various multipoles of the charge distribution with the applied potential [45, 49].

The electrostatic interaction energy  $U$  can be written as:

$$U = \int \rho(\vec{r}) \Phi(\vec{r}) d^3r, \quad (1.14)$$

where  $\Phi(\vec{r})$  is an applied potential. If  $\Phi(\vec{r})$  is a slowly varying external potential in a region where the charge distribution  $\rho(\vec{r})$  is non-vanishing, the potential  $\Phi(\vec{r})$  can be expanded in the Taylor series about  $\vec{r} = 0$  [42-44]:

$$U = q\Phi(0) - \vec{P} \cdot \vec{E}(0) - \frac{1}{6} \sum_i \sum_j Q_{ij} \frac{\partial E_j(0)}{\partial r_i} + \dots, \quad (1.15)$$

where  $q$ ,  $\vec{P}$  and  $Q_{ij}$  are defined in Section 1.7 (see Section 2.1), and  $\vec{E} = -\vec{\nabla}\Phi$ .

The expansion of the electrostatic interaction energy  $U$  in Eq. 1.15 shows the characteristic way that the charge distribution interacts with the external potential: a monopole with the potential (first term on the right-hand side), the dipole with the electric field (second term in the expansion), and the quadrupole with the electric field gradient (third term in the expansion), and so on. From Eq. 1.15, the expression for quadrupole-quadrupole interaction energy  $U_{quad}$  may be obtained:

$$U_{quad} = -\frac{1}{6} \sum_i \sum_j Q_{ij} \frac{\partial E_{quad}^j}{\partial r_i}, \quad (1.16)$$

which explicitly shows that the energy of a quadrupole moment in an external field depends on the spatial derivatives of the electric field components. The field gradient  $\partial E_{quad}^j / \partial r_i$  for a quadrupole field is calculated in Appendix A. The quadrupole interaction energy  $U_{quad}$  from Eq. 1.16 will be used in Section 2.12. The quadrupole interaction energy of a given charge distribution with an external potential is zero for the following cases: i) if the charge distribution is spherically symmetric, i.e.,  $Q_{ij} = 0$ , and ii) if the applied electric field is uniform, i.e.,  $\partial E_{quad}^j / \partial r_i = 0$ .

## 1.10 The long-range quadrupole-quadrupole interaction energy $U_{quad}$ formulation

The quadrupole potential  $\Phi_{quad}(\vec{r})$ , about the origin is the third term in the expansion of the potential,  $\Phi(\vec{r})$ , in Eq. 1.9:

$$\Phi_{quad}(\vec{r}) = \frac{1}{4\pi\epsilon_0} \frac{r_i Q'_{ij} r_j}{2r^5}, \quad (1.17)$$

where the prime is used to indicate a second quadrupole.

The electric field is the negative gradient of the potential:

$$\begin{aligned} E_{quad}^{\prime j} &= -\frac{\partial \Phi'_{quad}(\vec{r})}{\partial r_j} \\ &= \frac{1}{4\pi\epsilon_0} \frac{1}{2r^7} \left( 5r_j r_l Q'_{lm} r_m - 2r^2 r_l Q'_{lj} \right). \end{aligned} \quad (1.18)$$

The electric field gradient is expressed as:

$$\begin{aligned} 4\pi\epsilon_0 \frac{\partial E_{quad}^{\prime j}}{\partial r_i} &= -\frac{35}{2r^9} r_j r_l Q'_{lm} r_m r_i + \frac{1}{2r^7} \left( 10r_i Q'_{jl} r_l \right. \\ &\quad \left. + 10r_j Q'_{ii} r_l + \delta_{ij} r_l Q'_{lm} r_m - 2r^2 Q'_{ij} \right). \end{aligned} \quad (1.19)$$

See Appendix A.1 for detail. By combining Eqs. 1.16, 1.18 and 1.19, the quadrupole interaction energy can be expressed as:

$$\begin{aligned} 4\pi\epsilon_0 U_{quad} &= \frac{35}{12r^9} \sum_{ijlm} r_i Q_{ij} r_j r_l Q'_{lm} r_m - \frac{1}{6r^7} \left( \sum_{ijt} r_i Q_{ij} Q'_{jt} r_l \right. \\ &\quad \left. - r^2 \sum_{ij} Q_{ij} Q'_{ij} \right). \end{aligned} \quad (1.20)$$

For the two linear quadrupoles, Eq. 1.20 can be written as:

$$\begin{aligned} 4\pi\epsilon_0 U_{quad} &= \frac{35}{12r^9} \left( (x^2 Q_{11} + y^2 Q_{22} + z^2 Q_{33})(x^2 Q'_{11} + y^2 Q'_{22} + z^2 Q'_{33}) \right) \\ &\quad - \frac{5}{3r^7} \left( (xQ_{11} + yQ_{22} + zQ_{33})(xQ'_{11} + yQ'_{22} + zQ'_{33}) \right) \\ &\quad + \frac{1}{6r^5} \left( Q_{11} Q'_{11} + Q_{22} Q'_{22} + Q_{33} Q'_{33} \right), \end{aligned} \quad (1.21)$$

since all  $Q_{ij}$  and  $Q'_{ij}$  are zero for  $i \neq j$  for linear quadrupoles. From Eq. 1.21,  $U_{quad}$  can easily be calculated.

## 1.11 Quadrupole-quadrupole interaction energy $U_{quad}$ for the three different alignments of linear quadrupoles

Calculations of quadrupole interaction energy  $U_{quad}$  for the three different alignments of quadrupoles are carried out in this section. In each case, one of the quadrupoles is always fixed at the origin with its charges configured along the  $z$ -axis, and the other is selected arbitrarily along one of the coordinate axes.

### 1.11.1 Case I: Two quadrupoles aligned along the $z$ -axis

The coordinates of the center of the first and second quadrupoles are  $(0, 0, 0)$  and  $(0, 0, z)$ . The distance between the centers of quadrupoles is taken to be  $d$ . In this case, the charge distribution in both of the quadrupoles is symmetric to the  $z$ -axis. Since the quadrupoles considered herein are linear, all the off-diagonal components of the quadrupole moments associated with them vanishes, and only the diagonal components are non-zero. Fig. 1.5 shows such an alignment of the two quadrupoles along the  $z$ -axis. By using the symmetry of the charge distribution in both the quadrupoles, two relationships can be determined:

For quadrupole I,

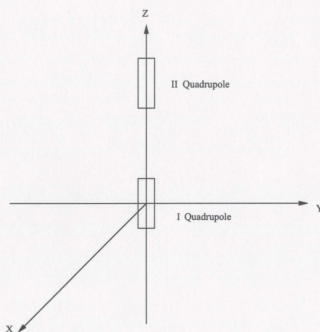
$$Q_{11} = Q_{22} = -\frac{Q_{33}}{2}$$

For quadrupole II,

$$Q'_{11} = Q'_{22} = -\frac{Q'_{33}}{2}.$$

From Eq. 1.21,  $U_{quad}^I$  for case I is:

$$U_{quad}^I = \frac{1}{4\pi\epsilon_0} \left( \frac{35}{12d^5} Q_{33} Q'_{33} - \frac{5}{3d^5} Q_{33} Q'_{33} + \frac{1}{4d^5} Q_{33} Q'_{33} \right)$$

Figure 1.5: Case I: Two quadrupoles aligned along the  $z$ -axis.

$$= \frac{1}{4\pi\epsilon_0} \left( \frac{3Q_{33}Q'_{33}}{2d^5} \right). \quad (1.22)$$

### 1.11.2 Case II: Two quadrupoles along the $x$ - and $z$ -axes

The coordinates of the centers of quadrupoles are  $(0, 0, 0)$  and  $(x, 0, 0)$  and the distance between them is taken to be  $d$ . The same arguments apply to this case as were used for case I, so that:

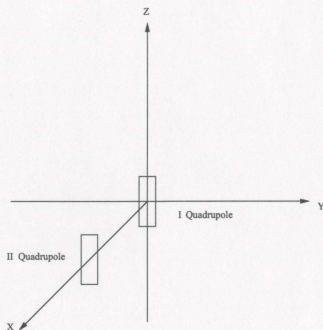
For quadrupole I,

$$Q_{11} = Q_{22} = -\frac{Q_{33}}{2}$$

For quadrupole II,

$$Q'_{11} = Q'_{22} = -\frac{Q'_{33}}{2}.$$

Fig. 1.6 shows a quadrupole at the origin and aligned along the  $z$ -axis, while the

Figure 1.6: Case II : Two quadrupoles along the  $x$ - and  $z$ -axes.

other is fixed along the  $x$ -axis with its charges configured parallel to the  $z$ -axis. The  $U_{quad}^{II}$  is calculated as:

$$\begin{aligned}
 U_{quad}^{II} &= \frac{1}{4\pi\epsilon_0} \left( -\frac{35}{12d^5} \frac{Q_{33}}{2} Q'_{11} + \frac{5}{3d^5} \frac{Q_{33}}{2} Q'_{11} + \frac{1}{4d^5} Q_{33} Q'_{33} \right) \\
 &= \frac{1}{4\pi\epsilon_0} \left( \frac{9Q_{33}Q'_{33}}{16d^5} \right).
 \end{aligned} \tag{1.23}$$

### 1.11.3 Case III: Two quadrupoles along the $y$ - and $z$ -axes

One of the quadrupoles is aligned along the  $y$ -axis and the other is aligned along the  $z$ -axis. The same argument apply to this case as was used for case I, so that:

For quadrupole I,

$$Q_{11} = Q_{22} = -\frac{Q_{33}}{2},$$

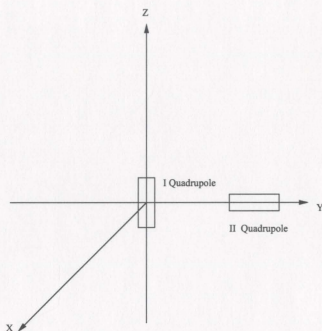


Figure 1.7: Case III : Two quadrupoles aligned along the  $y$ - and  $z$ -axes.

For quadrupole II,

$$Q'_{11} = Q'_{33} = -\frac{Q'_{22}}{2}.$$

Fig. 1.7 shows the mutually orthogonal alignments of the two quadrupoles. Taking the distance between quadrupoles to be  $d$ , the quadrupole interaction energy  $U_{quad}^{III}$  can be calculated as:

$$U_{quad}^{III} = -\frac{1}{4\pi\epsilon_0} \left( \frac{3Q_{33}Q'_{22}}{4d^5} \right). \quad (1.24)$$

The  $(-)$  sign indicates an attractive interaction, whereas the  $(+)$  sign obtained in cases I and II indicates repulsive interaction.

## 1.12 Organization of the present work

Chapter 2 is devoted to the calculations of quadrupole moment of the Pr  $4f^2$  electrons and of the transition metal ions displaced in a specific direction. The long-range quadrupole interaction energy between the Pr  $4f^2$  electrons and transition metal ions associated with the praseodymium-filled skutterudites under consideration will be calculated. Chapter 3 will provide a discussion and summary of the present work.



## Chapter 2

# Quadrupole Interactions in Filled Skutterudites

This chapter is devoted to the calculations of quadrupole moment due to the crystal field ground state of the Pr  $4f^2$  electrons. The quadrupole moment due to the displacement of T metal ions in a unique direction is also calculated, and the long-range quadrupole interactions between the Pr  $4f^2$  electrons and the displaced T metal ions are calculated for their three specific alignments.

### 2.1 Quadrupole moment calculation by using the Wigner-Eckart theorem

The quadrupole moment associated with the crystal field ground state  $|\Gamma_3^\pm\rangle$  of the Pr  $4f^2$  electrons can be calculated by using Eqs. 1.1, 1.6 and 1.7:

$$\begin{aligned} Q_{33} &= -e \langle \Gamma_3^\pm | 3z^2 - r^2 | \Gamma_3^\pm \rangle \\ &= B \langle \Gamma_3^\pm | (3J_z^2 - J^2) | \Gamma_3^\pm \rangle \end{aligned}$$

$$= \pm 8B\hbar^2, \quad (2.1)$$

where  $B$  is a proportionality constant. Similarly, the  $Q_{11}$  component is:

$$\begin{aligned} Q_{11} &= B \langle \Gamma_3^\pm | (3J_x^2 - J^2) | \Gamma_3^\pm \rangle \\ &= \mp 4B\hbar^2, \end{aligned} \quad (2.2)$$

and  $Q_{12} = Q_{23} = Q_{31} = 0$ . Tracelessness implies  $Q_{22} = \mp 4B$ . Hence, the quadrupole moment due to the crystal field ground state doublet  $|\Gamma_3^\pm\rangle$  of the Pr  $4f^2$  electrons resembles a linear quadrupole form (see Section 1.8).

Alternatively, the quadrupole moment associated with the crystal field ground state,  $|\Gamma_3^\pm\rangle$ , of the Pr  $4f^2$  electrons can be expressed as:

$$\begin{aligned} Q_{33} &= -e \int (3z^2 - r^2) \rho(\vec{r}) d^3r \\ &= -e\mathcal{A} \int_0^\pi \int_0^{2\pi} (3 \cos^2 \theta - 1) \rho(\theta, \phi) \sin \theta d\theta d\phi, \end{aligned} \quad (2.3)$$

where  $\rho(\vec{r})$  is the number density of charges of the Pr  $4f^2$  electrons,  $\mathcal{A}$  is the overall contribution from the radial part, and  $\rho(\theta, \phi)$  is the angular density of charges. The radial part  $\mathcal{A}$  has units of  $m^2$  and therefore  $Q_{33}$  has units of  $m^2C$ . The angular density  $\rho(\theta, \phi)$  of the Pr  $4f^2$  electrons will be calculated in Sections 2.7 and 2.8. An approximation for  $\mathcal{A}$  will be performed in Section 2.3.

By equating the results of Eq. 2.1 with Eq. 2.3, the characteristic parameter  $B$  can be obtained in terms of  $e\mathcal{A}$ . Once the value of  $B$  is known, the remaining components of the quadrupole moment can be calculated directly from the Wigner-Eckart theorem. This is done in Sections 2.5 and 2.6.

## 2.2 Approximation of the radial part $\mathcal{A}$ of the f-electron wave function

The maximum orbital radius  $R_{max}$  of the Pr  $4f^2$  electrons is approximately 40pm [50], where  $1\text{pm} = 10^{-12}\text{m}$ . Note that 40pm is a little less than one Bohr radius ( $0.53\text{\AA}$ ). A crude approximation of  $\mathcal{A}$  for the Pr  $4f^2$  electrons can be made such that the number density of electrons remains constant within a sphere of radius equivalent to  $R_{max}$ . The number density of a f-electron can be expressed as:

$$\rho(\vec{r}) = \rho(r)\rho(\theta, \phi), \quad (2.4)$$

where  $\rho(r)$  the radial part of the number density and  $\rho(\theta, \phi)$  is the angular part.  $\rho(\theta, \phi)$  is derived from the crystal field ground state, discussed in detail in Sections 2.4.3 and 2.5. There are two electrons in the system, therefore:

$$\int d^3r \rho(\vec{r}) = 2. \quad (2.5)$$

As shown in Section 2.5 (Eq. 2.35):

$$\int \rho(\theta, \phi) d\Omega = 2, \quad (2.6)$$

therefore

$$\int_0^\infty \rho(r) r^2 dr = 1. \quad (2.7)$$

The radial part  $\mathcal{A}$  defined in Eq. 2.3 is:

$$\mathcal{A} = \int_0^\infty \rho(r) r^4 dr. \quad (2.8)$$

Here,  $\rho(r)$  is approximated by a constant number  $C$  within the maximum orbital radius  $R_{max}$ , and is zero for  $r > R_{max}$ . Thus, Eq. 2.7 can be expressed as:

$$C \int_0^{R_{max}} r^2 dr = 1, \quad (2.9)$$

therefore,

$$C = \frac{3}{R_{max}^3}. \quad (2.10)$$

Then, from Eq. 2.8,  $\mathcal{A}$  is approximately,

$$\begin{aligned} \mathcal{A} &\approx \frac{3}{R_{max}^3} \int_0^{R_{max}} r^4 dr \\ &\approx \frac{3}{5} R_{max}^2 \\ &\approx 9.6 \times 10^{-22} \text{m}^2 \\ &\approx 960 \text{pm}^2. \end{aligned} \quad (2.11)$$

## 2.3 The Clebsch-Gordan decomposition of $J = 4$ Pr $4f^2$ electrons into $l_1 = 3$ , $l_2 = 3$ and $S = 1$

Hund's angular momentum for the Pr  $4f^2$  electrons is  $J = 4$ . The angular momentum state  $J = 4$  is decomposed to  $L = 5$  and  $S = 1$  states using the Clebsch-Gordan (C-G) decomposition method [36, 41]. The states  $L = 5$  and  $S = 1$  are decomposed into  $l_1 = 3$ ,  $l_2 = 3$ , and  $S = 1$  by the C-G decomposition method, as follows:

$$\begin{aligned} |5, \pm 5\rangle &= \pm \sqrt{\frac{1}{2}} \left( |3, \pm 3\rangle |3, \pm 2\rangle - |3, \pm 2\rangle |3, \pm 3\rangle \right) \\ |5, \pm 4\rangle &= \pm \sqrt{\frac{1}{2}} \left( |3, \pm 3\rangle |3, \pm 1\rangle - |3, \pm 1\rangle |3, \pm 3\rangle \right) \\ |5, \pm 3\rangle &= \pm \sqrt{\frac{1}{3}} \left( |3, \pm 3\rangle |3, 0\rangle - |3, 0\rangle |3, \pm 3\rangle \right) \pm \sqrt{\frac{1}{6}} \left( |3, \pm 2\rangle |3, \pm 1\rangle - |3, \pm 1\rangle |3, \pm 2\rangle \right) \\ |5, 2\rangle &= \sqrt{\frac{1}{6}} \left( |3, 3\rangle |3, -1\rangle - |3, -1\rangle |3, 3\rangle \right) + \sqrt{\frac{1}{3}} \left( |3, 2\rangle |3, 0\rangle - |3, 0\rangle |3, 2\rangle \right) \\ |5, 1\rangle &= \frac{1}{2} \sqrt{\frac{5}{21}} \left( |3, 3\rangle |3, -2\rangle - |3, -2\rangle |3, 3\rangle \right) + \frac{3}{2\sqrt{7}} \left( |3, 2\rangle |3, -1\rangle - |3, -1\rangle |3, 2\rangle \right) \\ &\quad + \sqrt{\frac{5}{42}} \left( |3, 1\rangle |3, 0\rangle - |3, 0\rangle |3, 1\rangle \right) \end{aligned}$$

$$\begin{aligned}
|5, 0\rangle &= \frac{1}{2\sqrt{21}} \left( |3, 3\rangle |3, -3\rangle - |3, -3\rangle |3, 3\rangle \right) + \frac{2}{\sqrt{21}} \left( |3, 2\rangle |3, -2\rangle - |3, -2\rangle |3, 2\rangle \right) \\
&\quad + \frac{5}{2\sqrt{21}} \left( |3, 1\rangle |3, -1\rangle - |3, -1\rangle |3, 1\rangle \right) \\
|5, -1\rangle &= \frac{1}{2}\sqrt{\frac{5}{21}} \left( |3, 2\rangle |3, -3\rangle - |3, -3\rangle |3, 2\rangle \right) + \frac{3}{2\sqrt{7}} \left( |3, 1\rangle |3, -2\rangle - |3, -2\rangle |3, 1\rangle \right) \\
&\quad + \sqrt{\frac{5}{42}} \left( |3, 0\rangle |3, -1\rangle - |3, -1\rangle |3, 0\rangle \right) \\
|5, -2\rangle &= \sqrt{\frac{1}{6}} \left( |3, 1\rangle |3, -3\rangle - |3, -3\rangle |3, 1\rangle \right) + \sqrt{\frac{1}{3}} \left( |3, 0\rangle |3, -2\rangle - |3, -2\rangle |3, 0\rangle \right) \quad (2.12)
\end{aligned}$$

On the RHS, the first factor in each product is  $|l_1, m_1\rangle$  and the second factor is  $|l_2, m_2\rangle$ .

Furthermore, the state  $J = 4$  can be decomposed into  $L = 5$  and  $S = 1$  using the Clebsch-Gordan decomposition method:

$$\begin{aligned}
|4, 4\rangle &= \frac{3}{\sqrt{11}} |5, 5\rangle |1, -1\rangle + \sqrt{\frac{1}{55}} |5, 3\rangle |1, 1\rangle - \frac{3}{\sqrt{55}} |5, 4\rangle |1, 0\rangle \\
|4, 2\rangle &= 2\sqrt{\frac{7}{55}} |5, 3\rangle |1, -1\rangle - \sqrt{\frac{21}{55}} |5, 2\rangle |1, 0\rangle + \sqrt{\frac{6}{55}} |5, 1\rangle |1, 1\rangle \\
|4, 0\rangle &= \sqrt{\frac{3}{11}} |5, 1\rangle |1, -1\rangle - \sqrt{\frac{5}{11}} |5, 0\rangle |1, 0\rangle + \sqrt{\frac{3}{11}} |5, -1\rangle |1, 1\rangle \\
|4, -2\rangle &= 2\sqrt{\frac{7}{55}} |5, -3\rangle |1, 1\rangle - \sqrt{\frac{21}{55}} |5, -2\rangle |1, 0\rangle + \sqrt{\frac{6}{55}} |5, -1\rangle |1, -1\rangle \\
|4, -4\rangle &= \frac{3}{\sqrt{11}} |5, -5\rangle |1, 1\rangle + \sqrt{\frac{1}{55}} |5, -3\rangle |1, -1\rangle - \frac{3}{\sqrt{55}} |5, -4\rangle |1, 0\rangle, \quad (2.13)
\end{aligned}$$

where on the RHS, the first factor is  $|l, m\rangle$  as shown in Eq. 2.13 and the second factor is  $|S, M_S\rangle$ . Combining Eqs. 2.12 and 2.13:

$$\begin{aligned}
|4, 2\rangle &= 2\sqrt{\frac{7}{55}} \left[ \sqrt{\frac{1}{3}} (|3, 3\rangle |3, 0\rangle - |3, 0\rangle |3, 3\rangle) \right. \\
&\quad \left. + \sqrt{\frac{1}{6}} (|3, 2\rangle |3, 1\rangle - |3, 1\rangle |3, 2\rangle) \right] |1, -1\rangle \\
&\quad - \sqrt{\frac{21}{55}} \left[ \sqrt{\frac{1}{6}} (|3, 3\rangle |3, -1\rangle - |3, -1\rangle |3, 3\rangle) \right. \\
&\quad \left. + \sqrt{\frac{1}{3}} (|3, 2\rangle |3, 0\rangle - |3, 0\rangle |3, 2\rangle) \right] |1, 0\rangle
\end{aligned}$$

$$\begin{aligned}
& +\sqrt{\frac{6}{55}} \left( \frac{1}{2} \sqrt{\frac{5}{21}} (|3, 3\rangle |3, -2\rangle - |3, -2\rangle |3, 3\rangle) \right. \\
& +\frac{3}{2\sqrt{7}} (|3, 2\rangle |3, -1\rangle - |3, -1\rangle |3, 2\rangle) \\
& \left. +\sqrt{\frac{5}{42}} (|3, 1\rangle |3, 0\rangle - |3, 0\rangle |3, 1\rangle) \right) |1, 1\rangle. \quad (2.14)
\end{aligned}$$

On the RHS, the first factor is  $|l_1, m_1\rangle$ , the second factor is  $|l_2, m_2\rangle$  and the third factor is  $|S, M_s\rangle$ . Note that the spin part is in the triplet state, which is symmetric under exchange. The orbital part is clearly antisymmetric.

Eq. 2.14 is an example of how the  $J = 4$  state of the Pr  $4f^2$  electrons decompose into  $l_1 = 3$ ,  $l_2 = 3$  and  $S = 1$  states by means of C-G decomposition. All the remaining states of  $J = 4$  will follow the same pattern as for Eq. 2.14. In particular, we will consider the crystal field ground state  $|\Gamma_3^- \rangle$  of the Pr  $4f^2$  electrons as defined in Eq. 1.1 by using Eq. 2.14 and its similar pattern.

## 2.4 Angular charge density formulation

Prior to determining the wave function of the Pr  $4f^2$  electrons, which possess both space and spin, the wave functions for a single spin 1/2 particle, and a system of two spin-less particles will be discussed.

### 2.4.1 Wave function for one spin 1/2 particle

If  $\Psi(\vec{r})$  is the state function of a single electron, the probability of finding it at position  $\vec{r}$  is  $\rho(\vec{r}) = |\Psi(\vec{r})|^2$ . The total probability of finding a single electron at a given position is one:

$$\int \rho(\vec{r}) d^3r = 1. \quad (2.15)$$

Let  $\psi_\uparrow(\vec{r})$  and  $\psi_\downarrow(\vec{r})$  be wave functions for the spin up and down components

respectively. The probability of finding the particle with spin up at position  $\vec{r}$  is:

$$\rho_{\uparrow}(\vec{r}) = |\psi_{\uparrow}(\vec{r})|^2,$$

and the probability of finding the particle with spin down at position  $\vec{r}$  is:

$$\rho_{\downarrow}(\vec{r}) = |\psi_{\downarrow}(\vec{r})|^2.$$

The total probability density of the particle having either spin up or down at position  $\vec{r}$  is:

$$\begin{aligned} \rho_{total}(\vec{r}) &= \rho_{\uparrow}(\vec{r}) + \rho_{\downarrow}(\vec{r}) \\ &= |\psi_{\uparrow}(\vec{r})|^2 + |\psi_{\downarrow}(\vec{r})|^2, \end{aligned} \quad (2.16)$$

and the probability of finding the particle with spin up or down at any position is:

$$\int (\rho_{\uparrow}(\vec{r}) + \rho_{\downarrow}(\vec{r})) d^3r = 1, \quad (2.17)$$

which is consistent with the normalization condition.

## 2.4.2 Wave function for two spin-less particles

Let us consider a spin-less two particles wave function of the form:

$$\Psi(\vec{r}_1, \vec{r}_2) = \psi_1(\vec{r}_1)\psi_2(\vec{r}_2), \quad (2.18)$$

where the normalization condition is:

$$\int |\Psi(\vec{r}_1, \vec{r}_2)|^2 d^3r_1 d^3r_2 = 1.$$

The wave functions  $\psi_1(\vec{r}_1)$  and  $\psi_2(\vec{r}_2)$  each satisfy the normalization conditions:

$$\int |\psi_1(\vec{r}_1)|^2 d^3r_1 = 1$$

and

$$\int |\psi_2(\vec{r}_2)|^2 d^3 r_2 = 1.$$

The probability of finding the particle 1 at the position  $\vec{r}_1$  with particle 2 anywhere is:

$$\begin{aligned} \rho_1(\vec{r}_1) &= |\psi_1(\vec{r}_1)|^2 \int |\psi_2(\vec{r}_2)|^2 d^3 r_2 \\ &= |\psi_1(\vec{r}_1)|^2, \end{aligned} \quad (2.19)$$

since the probability of finding the second particle anywhere is one. The probability of finding particle 2 at position  $\vec{r}_2$  with particle 1 anywhere is:

$$\rho_2(\vec{r}_2) = |\psi_2(\vec{r}_2)|^2. \quad (2.20)$$

The number density of the two spin-less particles at position  $\vec{r}$  is therefore:

$$\begin{aligned} \rho(\vec{r}) &= \rho_1(\vec{r}) + \rho_2(\vec{r}) \\ &= |\psi_1(\vec{r})|^2 + |\psi_2(\vec{r})|^2. \end{aligned} \quad (2.21)$$

Hence the total number of particles is:

$$\int \rho(\vec{r}) d^3 r = 2, \quad (2.22)$$

as expected.

In general, the spin-less two particle wave function is more complicated:

$$\Psi(\vec{r}_1, \vec{r}_2) = \sum_{\alpha\beta} K_{\alpha\beta} \psi_\alpha(\vec{r}_1) \psi_\beta(\vec{r}_2), \quad (2.23)$$

where  $\psi_\alpha$  and  $\psi_\beta$  are orthonormal functions, and for fermions,  $K_{\alpha\beta} = -K_{\beta\alpha}$  i.e. because of antisymmetric property of fermions. The latter condition ensures that the wave function is odd under the exchange of particles. The probability of finding the first particle at  $\vec{r}_1$  and the second particle at  $\vec{r}_2$  is:

$$|\Psi(\vec{r}_1, \vec{r}_2)|^2 = \sum_{\alpha\beta\gamma\delta} K_{\alpha\beta} \psi_\alpha(\vec{r}_1) \psi_\beta(\vec{r}_2) K_{\gamma\delta} \psi_\gamma^*(\vec{r}_1) \psi_\delta^*(\vec{r}_2). \quad (2.24)$$



The probability of finding the first particle at  $\vec{r}_1$  with the second particle anywhere is:

$$\begin{aligned}
 \rho_1(\vec{r}_1) &= \int |\Psi(\vec{r}_1, \vec{r}_2)|^2 d^3r_2 \\
 &= \sum_{\alpha\beta\gamma\delta} K_{\alpha\beta} K_{\gamma\delta} \psi_\alpha(\vec{r}_1) \psi_\gamma^*(\vec{r}_1) \int d^3r_2 \psi_\beta(\vec{r}_2) \psi_\delta^*(\vec{r}_2) \\
 &= \sum_{\alpha\beta\gamma\delta} K_{\alpha\beta} K_{\gamma\delta} \psi_\alpha(\vec{r}_1) \psi_\gamma^*(\vec{r}_1) \delta_{\beta\delta} \\
 &= \sum_{\alpha\beta\gamma} K_{\alpha\beta} K_{\gamma\beta} \psi_\alpha(\vec{r}_1) \psi_\gamma^*(\vec{r}_1). \tag{2.25}
 \end{aligned}$$

Similarly, the probability of finding the second particle at a position  $\vec{r}_2$  with the first particle anywhere is:

$$\rho_2(\vec{r}_2) = \sum_{\alpha\beta\gamma} K_{\alpha\beta} K_{\gamma\beta} \psi_\alpha(\vec{r}_2) \psi_\gamma^*(\vec{r}_2). \tag{2.26}$$

The number density of particles at position  $\vec{r}$  is:

$$\begin{aligned}
 \rho(\vec{r}) &= \rho_1(\vec{r}) + \rho_2(\vec{r}) \\
 &= 2 \sum_{\alpha\beta\gamma} K_{\alpha\beta} K_{\gamma\beta} \psi_\alpha(\vec{r}) \psi_\gamma^*(\vec{r}) \\
 &= -2 \sum_{\alpha\beta\gamma} K_{\alpha\beta} K_{\beta\gamma} \psi_\alpha(\vec{r}) \psi_\gamma^*(\vec{r}) \\
 &= -2 \sum_{\alpha\gamma} \psi_\alpha(\vec{r}) [K^2]_{\alpha\gamma} \psi_\gamma^*(\vec{r}). \tag{2.27}
 \end{aligned}$$

### 2.4.3 Wave function for two particles with spin

To include the effect of spin, the probabilities of finding particles in different spin states are added because the different spin states are orthogonal. The spin states may be the eigenstate of either the total spin  $S = S_1 + S_2$  (i.e.  $S^2$  and  $S_z$ ) or they may be eigenstates of  $S_1$  and  $S_2$  separately (i.e.  $S_{1z}$  and  $S_{2z}$ ). We choose the former.

The wavefunction can be written as [51]:

$$\Psi(\vec{r}_1, \vec{r}_2, SM_S) = \psi(\vec{r}_1, \vec{r}_2) |SM_S\rangle. \tag{2.28}$$

Because the electrons are in the spin  $S = 1$  state, which is symmetric, and the antisymmetric form of the space part as in Eq. 2.23 is valid.

The angular charge density  $\rho(\theta, \phi)$  of the Pr  $4f^2$  electrons in states  $|\Gamma_3^\pm\rangle$  is calculated by using Eq. 2.27 where  $\rho(\theta, \phi)$  can be expressed as follows:

$$\rho(\theta, \phi) = -2 \begin{pmatrix} Y_3^3 & Y_3^2 & Y_3^1 & Y_3^0 & Y_3^{-1} & Y_3^{-2} & Y_3^{-3} \end{pmatrix} [K^2] \begin{pmatrix} Y_3^{3*} \\ Y_3^{2*} \\ Y_3^{1*} \\ Y_3^{0*} \\ Y_3^{-1*} \\ Y_3^{-2*} \\ Y_3^{-3*} \end{pmatrix}. \quad (2.29)$$

Note that the spherical harmonics  $Y_l^m$  correspond to the kets  $|l, m\rangle$ .

The states  $|\Gamma_3^+\rangle$  and  $|\Gamma_3^-\rangle$  are expressed in terms of  $l_1 = 3$ ,  $l_2 = 3$  and  $S = 1$  according to Eqs. 1.1 and 2.13. In the following section, three different matrices  $K(1, 1)$ ,  $K(1, 0)$  and  $K(1, -1)$  are found for each of the  $|1, 1\rangle$ ,  $|1, 0\rangle$  and  $|1, -1\rangle$  spin states respectively.  $K^2$  is the sum  $[K(1, 1)]^2 + [K(1, 0)]^2 + [K(1, -1)]^2$ , which corresponds to adding the probabilities of the three different spin states.

## 2.5 Quadrupole moment possessed by the Pr $4f^2$ electrons in $|\Gamma_3^-\rangle$ and $|\Gamma_3^+\rangle$ states

The crystal field ground state  $|\Gamma_3^-\rangle$  (Eq. 1.1) may be expanded using Eq. 2.13:

$$\begin{aligned} |\Gamma_3^-\rangle &= \frac{1}{\sqrt{2}}(|4, 2\rangle + |4, -2\rangle) \\ &= \sqrt{\frac{14}{55}} |5, 3\rangle |1, -1\rangle + \sqrt{\frac{21}{110}} |5, 2\rangle |1, 0\rangle + \sqrt{\frac{3}{55}} |5, 1\rangle |1, 1\rangle \end{aligned}$$

$$\begin{aligned}
& + \sqrt{\frac{3}{55}} |5, -1\rangle |1, -1\rangle + \sqrt{\frac{14}{55}} |5, -3\rangle |1, 1\rangle - \sqrt{\frac{21}{110}} |5, -2\rangle |1, 0\rangle \\
= & \left[ \sqrt{\frac{14}{55}} |5, 3\rangle + \sqrt{\frac{3}{55}} |5, -1\rangle \right] |1, -1\rangle - \left[ \sqrt{\frac{21}{110}} |5, -2\rangle + \sqrt{\frac{21}{110}} |5, 2\rangle \right] |1, 0\rangle \\
& + \left[ \sqrt{\frac{3}{55}} |5, 1\rangle + \sqrt{\frac{14}{55}} |5, -3\rangle \right] |1, 1\rangle. \tag{2.30}
\end{aligned}$$

This is further expanded using Eq. 2.12:

$$\begin{aligned}
|\Gamma_3^-\rangle = & \sqrt{\frac{1}{55}} \left[ \sqrt{\frac{14}{3}} (|3, 3\rangle |3, 0\rangle - |3, 0\rangle |3, 3\rangle) + \sqrt{\frac{7}{3}} (|3, 2\rangle |3, 1\rangle - |3, 1\rangle |3, 2\rangle) \right. \\
& + \frac{1}{2} \sqrt{\frac{5}{7}} (|3, 2\rangle |3, -3\rangle - |3, -3\rangle |3, 2\rangle) + \frac{3}{2} \sqrt{\frac{3}{7}} (|3, 1\rangle |3, -2\rangle - |3, -2\rangle |3, 1\rangle) \\
& \left. + \sqrt{\frac{5}{14}} (|3, 0\rangle |3, -1\rangle - |3, -1\rangle |3, 0\rangle) \right] |1, -1\rangle \\
& - \sqrt{\frac{21}{110}} \left[ \sqrt{\frac{1}{6}} (|3, 1\rangle |3, -3\rangle - |3, -3\rangle |3, 1\rangle) + \sqrt{\frac{1}{3}} (|3, 0\rangle |3, -2\rangle - |3, -2\rangle |3, 0\rangle) \right. \\
& \left. + \sqrt{\frac{1}{6}} (|3, 3\rangle |3, -1\rangle - |3, -1\rangle |3, 3\rangle) + \sqrt{\frac{1}{3}} (|3, 2\rangle |3, 0\rangle - |3, 0\rangle |3, 2\rangle) \right] |1, 0\rangle \\
& + \sqrt{\frac{1}{55}} \left[ \frac{1}{2} \sqrt{\frac{5}{7}} (|3, 3\rangle |3, -2\rangle - |3, -2\rangle |3, 3\rangle) + \frac{3}{2} \sqrt{\frac{3}{7}} (|3, 2\rangle |3, -1\rangle \right. \\
& - |3, -1\rangle |3, 2\rangle) + \sqrt{\frac{5}{14}} (|3, 1\rangle |3, 0\rangle - |3, 0\rangle |3, 1\rangle) + \sqrt{\frac{14}{3}} (|3, 0\rangle |3, -3\rangle \\
& \left. - |3, -3\rangle |3, 0\rangle) + \sqrt{\frac{7}{3}} (|3, -1\rangle |3, -2\rangle - |3, -2\rangle |3, -1\rangle) \right] |1, 1\rangle. \tag{2.31}
\end{aligned}$$

Just as in Eq. 2.14, the first factor is  $|l_1, m_1\rangle$ , the second factor is  $|l_2, m_2\rangle$  and the third factor is  $|S, M_s\rangle$ .

Extracting the matrices  $K(1, 1)$ ,  $K(1, 0)$  and  $K(1, -1)$  from Eq. 2.31 from the coefficients of spin states  $|1, 1\rangle$ ,  $|1, 0\rangle$  and  $|1, -1\rangle$  is the first step in order to perform the number density calculations. Each of the  $K(S, M_S)$  matrices are of the order  $7 \times 7$ . The matrix  $K(1, 1)$  can be found from the coefficient of spin function  $|1, 1\rangle$  from

Eq. 2.31:

$$K(1, 1) = \begin{pmatrix} 0 & 0 & 0 & 0 & 0 & \frac{1}{2\sqrt{77}} & 0 \\ 0 & 0 & 0 & 0 & \frac{3}{2}\sqrt{\frac{3}{385}} & 0 & 0 \\ 0 & 0 & 0 & \frac{1}{\sqrt{154}} & 0 & 0 & 0 \\ 0 & 0 & -\frac{1}{\sqrt{154}} & 0 & 0 & 0 & \sqrt{\frac{14}{165}} \\ 0 & -\frac{3}{2}\sqrt{\frac{3}{385}} & 0 & 0 & 0 & \sqrt{\frac{7}{165}} & 0 \\ -\frac{1}{2\sqrt{77}} & 0 & 0 & 0 & -\sqrt{\frac{7}{165}} & 0 & 0 \\ 0 & 0 & 0 & -\sqrt{\frac{14}{165}} & 0 & 0 & 0 \end{pmatrix}$$

and

$$K(1, 1)^2 = \begin{pmatrix} -\frac{1}{308} & 0 & 0 & 0 & -\frac{1}{22\sqrt{15}} & 0 & 0 \\ 0 & -\frac{27}{1540} & 0 & 0 & 0 & \frac{3}{110} & 0 \\ 0 & 0 & -\frac{1}{154} & 0 & 0 & 0 & \frac{1}{11\sqrt{15}} \\ 0 & 0 & 0 & -\frac{211}{2310} & 0 & 0 & 0 \\ -\frac{1}{22\sqrt{15}} & 0 & 0 & 0 & -\frac{277}{4620} & 0 & 0 \\ 0 & \frac{3}{110} & 0 & 0 & 0 & -\frac{211}{4620} & 0 \\ 0 & 0 & \frac{1}{11\sqrt{15}} & 0 & 0 & 0 & -\frac{14}{165} \end{pmatrix}$$

The matrix  $K(1, -1)$  can be found from the coefficient of spin function  $|1, -1\rangle$  from Eq. 2.31:

$$K(1, -1) = \begin{pmatrix} 0 & 0 & 0 & \sqrt{\frac{14}{165}} & 0 & 0 & 0 \\ 0 & 0 & \sqrt{\frac{7}{165}} & 0 & 0 & 0 & \frac{1}{2\sqrt{77}} \\ 0 & -\sqrt{\frac{7}{165}} & 0 & 0 & 0 & \frac{3}{2}\sqrt{\frac{3}{385}} & 0 \\ -\sqrt{\frac{14}{165}} & 0 & 0 & 0 & \frac{1}{\sqrt{154}} & 0 & 0 \\ 0 & 0 & 0 & -\frac{1}{\sqrt{154}} & 0 & 0 & 0 \\ 0 & 0 & -\frac{3}{2}\sqrt{\frac{3}{385}} & 0 & 0 & 0 & 0 \\ 0 & -\frac{1}{2\sqrt{77}} & 0 & 0 & 0 & 0 & 0 \end{pmatrix}$$

and

$$K(1, -1)^2 = \begin{pmatrix} -\frac{14}{165} & 0 & 0 & 0 & \frac{1}{11\sqrt{15}} & 0 & 0 \\ 0 & -\frac{211}{4620} & 0 & 0 & 0 & \frac{3}{110} & 0 \\ 0 & 0 & -\frac{277}{4620} & 0 & 0 & 0 & -\frac{1}{22\sqrt{15}} \\ 0 & 0 & 0 & 0 & -\frac{211}{2310} & 0 & 0 \\ \frac{1}{11\sqrt{15}} & 0 & 0 & 0 & -\frac{1}{154} & 0 & 0 \\ 0 & \frac{3}{110} & 0 & 0 & 0 & -\frac{27}{1540} & 0 \\ 0 & 0 & -\frac{1}{22\sqrt{15}} & 0 & 0 & 0 & \frac{1}{308} \end{pmatrix}.$$

The matrix  $K(1, 0)$  can be written from the coefficient of spin function  $|1, 0\rangle$  from Eq. 2.31:

$$K(1, 0) = \begin{pmatrix} 0 & 0 & 0 & 0 & -\frac{1}{2}\sqrt{\frac{7}{55}} & 0 & 0 \\ 0 & 0 & 0 & -\sqrt{\frac{7}{110}} & 0 & 0 & 0 \\ 0 & 0 & 0 & 0 & 0 & 0 & -\frac{1}{2}\sqrt{\frac{7}{55}} \\ 0 & \sqrt{\frac{7}{110}} & 0 & 0 & 0 & -\sqrt{\frac{7}{110}} & 0 \\ \frac{1}{2}\sqrt{\frac{7}{55}} & 0 & 0 & 0 & 0 & 0 & 0 \\ 0 & 0 & 0 & \sqrt{\frac{7}{110}} & 0 & 0 & 0 \\ 0 & 0 & \frac{1}{2}\sqrt{\frac{7}{55}} & 0 & 0 & 0 & 0 \end{pmatrix}$$

and

$$K(1, 0)^2 = \begin{pmatrix} -\frac{7}{220} & 0 & 0 & 0 & 0 & 0 & 0 \\ 0 & -\frac{7}{110} & 0 & 0 & 0 & \frac{7}{110} & 0 \\ 0 & 0 & -\frac{7}{220} & 0 & 0 & 0 & 0 \\ 0 & 0 & 0 & 0 & -\frac{7}{55} & 0 & 0 \\ 0 & 0 & 0 & 0 & -\frac{7}{220} & 0 & 0 \\ 0 & \frac{7}{110} & 0 & 0 & 0 & -\frac{7}{110} & 0 \\ 0 & 0 & 0 & 0 & 0 & 0 & -\frac{7}{220} \end{pmatrix}.$$

Obviously, the matrices  $K(1, 1)$ ,  $K(1, 0)$  and  $K(1, -1)$  are all antisymmetric. Using the formula:  $K^2 = K(1, 1)^2 + K(1, -1)^2 + K(1, 0)^2$  yields:

$$K^2 = \begin{pmatrix} -\frac{277}{2310} & 0 & 0 & 0 & \frac{1}{22\sqrt{15}} & 0 & 0 \\ 0 & -\frac{293}{2310} & 0 & 0 & 0 & \frac{13}{110} & 0 \\ 0 & 0 & -\frac{227}{2310} & 0 & 0 & 0 & \frac{1}{22\sqrt{15}} \\ 0 & 0 & 0 & -\frac{716}{2310} & 0 & 0 & 0 \\ \frac{1}{22\sqrt{15}} & 0 & 0 & 0 & -\frac{227}{2310} & 0 & 0 \\ 0 & \frac{13}{110} & 0 & 0 & 0 & -\frac{293}{2310} & 0 \\ 0 & 0 & \frac{1}{22\sqrt{15}} & 0 & 0 & 0 & -\frac{277}{2310} \end{pmatrix}. \quad (2.32)$$

From Eq. 2.32, the trace of  $K^2$  is  $-1$ , hence  $\text{Tr}(K^T K) = 1$ , which indicates that the wave functions used in Eq. 2.29 are normalized. The number density of the Pr  $4f^2$  electrons can be calculated by substituting  $K^2$  from Eq. 2.32 into Eq. 2.29:

$$\rho(\vec{r}) = -2\rho(r) \begin{pmatrix} Y_3^3 & Y_3^2 & Y_3^1 & Y_3^0 & Y_3^{-1} & Y_3^{-2} & Y_3^{-3} \end{pmatrix} \begin{pmatrix} -\frac{277}{2310} & 0 & 0 & 0 & \frac{1}{22\sqrt{15}} & 0 & 0 \\ 0 & -\frac{293}{2310} & 0 & 0 & 0 & \frac{13}{110} & 0 \\ 0 & 0 & -\frac{227}{2310} & 0 & 0 & 0 & \frac{1}{22\sqrt{15}} \\ 0 & 0 & 0 & -\frac{716}{2310} & 0 & 0 & 0 \\ \frac{1}{22\sqrt{15}} & 0 & 0 & 0 & -\frac{227}{2310} & 0 & 0 \\ 0 & \frac{13}{110} & 0 & 0 & 0 & -\frac{293}{2310} & 0 \\ 0 & 0 & \frac{1}{22\sqrt{15}} & 0 & 0 & 0 & -\frac{277}{2310} \end{pmatrix} \begin{pmatrix} Y_3^{3*} \\ Y_3^{2*} \\ Y_3^{1*} \\ Y_3^{0*} \\ Y_3^{-1*} \\ Y_3^{-2*} \\ Y_3^{-3*} \end{pmatrix}, \quad (2.33)$$

where  $\rho(r)$  is the contribution of radial part to the number density. Further simplifying Eq. 2.33:

$$\rho(\vec{r}) = -2\rho(r) \left[ -\frac{277}{2310} Y_3^3 Y_3^{3*} + \frac{1}{22\sqrt{15}} Y_3^{-1} Y_3^{3*} - \frac{293}{2310} Y_3^2 Y_3^{2*} + \frac{13}{110} Y_3^{-2} Y_3^{2*} \right. \\ \left. - \frac{227}{2310} Y_3^1 Y_3^{1*} + \frac{1}{22\sqrt{15}} Y_3^{-3} Y_3^{-1*} - \frac{716}{2310} Y_3^0 Y_3^{0*} - \frac{227}{2310} Y_3^{-1} Y_3^{-1*} \right]$$

$$\begin{aligned}
& + \frac{1}{22\sqrt{15}} Y_3^3 Y_3^{-1*} - \frac{293}{2310} Y_3^{-2} Y_3^{-2*} + \frac{13}{110} Y_3^2 Y_3^{-2*} \\
& - \left. \frac{277}{2310} Y_3^{-3} Y_3^{-3*} + \frac{1}{22\sqrt{15}} Y_3^1 Y_3^{-3*} \right) \\
= & \rho(r) \left( \left( \frac{1108}{2310} |Y_3^3|^2 + \frac{1172}{2310} |Y_3^2|^2 + \frac{908}{2310} |Y_3^1|^2 + \frac{1432}{2310} |Y_3^0|^2 \right) \right. \\
& - \frac{1}{11\sqrt{15}} (Y_3^{-1} Y_3^{3*} + Y_3^{-3} Y_3^{1*} + Y_3^3 Y_3^{-1*} + Y_3^1 Y_3^{-3*}) \\
& \left. - \frac{13}{55} (Y_3^{-2} Y_3^{2*} + Y_3^2 Y_3^{-2*}) \right) \\
= & \rho(r) \frac{1}{\pi} \left( \left( \frac{1033}{2640} + \frac{19}{10} \cos^2 \theta - \frac{1085}{176} \cos^4 \theta + \frac{119}{24} \cos^6 \theta \right) \right. \\
& \left. - \frac{7}{176} \cos 4\phi \sin^4 \theta (34 \cos^2 \theta + 1) \right), \tag{2.34}
\end{aligned}$$

where the spherical harmonics for  $l = 3$  are given in Appendix A.2.

The total number of electrons calculated by using their number density should be 2 for the Pr  $4f^2$  electrons:

$$\begin{aligned}
\int_0^{2\pi} \int_0^\pi \rho(\theta, \phi) \sin \theta d\theta d\phi &= \frac{1}{\pi} \int_0^{2\pi} \int_0^\pi \left( \left( \frac{1033}{2640} + \frac{19}{10} \cos^2 \theta - \frac{1085}{176} \cos^4 \theta + \frac{119}{24} \cos^6 \theta \right) \right. \\
& \left. - \frac{7}{176} \cos 4\phi \sin^4 \theta (34 \cos^2 \theta + 1) \right) \sin \theta d\theta d\phi \\
&= 4(0.3912 + 0.6333 - 1.2329 + 0.7083) \\
&= 2, \tag{2.35}
\end{aligned}$$

as expected. Note that the contribution due to the second integral is zero because

$$\int_0^{2\pi} \cos 4\phi d\phi = 0.$$

The quadrupole moment due to the Pr  $4f^2$  electrons along the z-axis is:

$$\begin{aligned}
Q_{33} &= -e \int (3z^2 - r^2) \rho(\vec{r}) d^3r \\
&= -e \int (3z^2 - r^2) \rho(r) \rho(\theta, \phi) r^2 dr \sin \theta d\theta d\phi \\
&= -eA \int_0^{2\pi} \int_0^\pi (3\cos^2 \theta - 1) \rho(\theta, \phi) \sin \theta d\theta d\phi \\
&= -eA \frac{1}{\pi} \int_0^{2\pi} \int_0^\pi (3\cos^2 \theta - 1) \left( \left( \frac{1033}{2640} + \frac{19}{10} \cos^2 \theta - \frac{1085}{176} \cos^4 \theta \right) \right.
\end{aligned}$$

$$\begin{aligned}
& + \frac{119}{24} \cos^6 \theta - \frac{7}{176} \sin^4 \theta (34 \cos^2 \theta + 1) \cos 4\phi \Big) \sin \theta d\theta d\phi \\
= & -e\mathcal{A} \int_0^\pi \left( -2 \left( -\frac{1033}{2640} - \frac{639}{880} \cos^2 \theta + \frac{10441}{880} \cos^4 \theta \right. \right. \\
& \left. \left. - \frac{12383}{528} \cos^6 \theta + \frac{119}{8} \cos^8 \theta \right) d \cos \theta \right) \\
= & -4e\mathcal{A} (-0.391287878 - 0.242045454 + 2.372954545 \\
& - 3.350378788 + 1.652777778) \\
= & -0.168080811e\mathcal{A}, \tag{2.36}
\end{aligned}$$

where the radial part of the charge distribution  $\mathcal{A}$  is defined in Eq. 2.8.

By substituting the approximation of  $\mathcal{A}$  from Eq. 2.11 into Eq. 2.36, an approximate value of  $Q_{33}$  for the Pr  $4f^2$  electrons in the ground state  $|\Gamma_3^- \rangle$  can be calculated as:

$$Q_{33} \approx -2.6 \times 10^{-41} \text{m}^2 \text{C} \approx -2.6 \times 10^{-17} \text{pm}^2 \text{C}. \tag{2.37}$$

The components of the quadrupole moment  $Q_{ij}$  associated with the Pr  $4f^2$  electrons in the states  $|\Gamma_3^- \rangle$  or  $|\Gamma_3^+ \rangle$  can be calculated by using the Wigner-Eckart theorem, which is discussed in Section 1.6.  $Q_{33}$  has been calculated by this method in Eq. 2.1 for the electrons in states  $|\Gamma_3^- \rangle$  and  $|\Gamma_3^+ \rangle$ , and associated quadrupole moments are  $\mp 8B\hbar^2$  where  $B$  is a proportionality constant. Comparing Eqs. 2.1 and 2.36, we find:

$$-8B\hbar^2 = -0.168080811e\mathcal{A}. \tag{2.38}$$

Using the approximate value of  $\mathcal{A}$  from Eq. 2.11 yields:

$$\hbar^2 B \approx 3.2 \times 10^{-42} \text{m}^2 \text{C}.$$

With the value of  $B$  for the Pr  $4f^2$  electrons in the ground state  $|\Gamma_3^- \rangle$  or  $|\Gamma_3^+ \rangle$ , i.e.,  $J = 4$ , one can apply the Wigner-Eckart theorem to calculate the other components of  $Q_{ij}$  directly. The quadrupole component  $Q_{22}$  is calculated via the Wigner-Eckart



theorem using the value of  $B$  from Eq. 2.38:

$$\begin{aligned} Q_{22} &= B \langle \Gamma_3^- | (3J_y^2 - J^2) | \Gamma_3^- \rangle \\ &= 4B\hbar^2 \\ &\approx 1.3 \times 10^{-41} \text{m}^2\text{C}. \end{aligned} \quad (2.39)$$

Similarly,  $Q_{ij} = 0$  for  $i \neq j$ , and  $Q_{11} = Q_{22}$ .

Using the Wigner-Eckart theorem the quadrupole moment  $Q_{33}$  of  $|\Gamma_3^+\rangle$  state is:

$$Q_{33} = 0.168080811e\mathcal{A}. \quad (2.40)$$

This result was verified by performing a similar lengthy calculation as for  $|\Gamma_3^-\rangle$ .

## 2.6 Quadrupole moment due to the displacement of T metal ions

The present section is devoted to the calculation of the quadrupole moment due to the displacement of T metal ions. A particular displacement of Fe/Ru ions in  $\text{PrFe}_4\text{P}_{12}$  produces a crystal field which splits the Pr  $4f^2$  ground state doublet into non-magnetic states of opposite quadrupole moments [4]. In this section we shall show that such a displacement also possesses a quadrupole moment.

In a bcc unit cell of a filled skutterudite, the positions of two Pr ions are  $(0, 0, 0)$  and  $(\frac{a}{2}, \frac{a}{2}, \frac{a}{2})$ . As discussed in chapter 1, the T metal ions are positioned midway between praseodymium ions. The initial positions of eight T metal ions in a bcc unit cell that is shifted so that the point  $(0, 0, 0)$  lies in the center, are the corners of a cube,

$$\begin{aligned} \left(\frac{a}{4}, \frac{a}{4}, \frac{a}{4}\right), \left(\frac{a}{4}, \frac{a}{4}, -\frac{a}{4}\right), \left(\frac{a}{4}, -\frac{a}{4}, \frac{a}{4}\right), \left(-\frac{a}{4}, \frac{a}{4}, \frac{a}{4}\right), \left(\frac{a}{4}, -\frac{a}{4}, -\frac{a}{4}\right), \\ \left(-\frac{a}{4}, -\frac{a}{4}, \frac{a}{4}\right), \left(-\frac{a}{4}, \frac{a}{4}, -\frac{a}{4}\right), \left(-\frac{a}{4}, -\frac{a}{4}, -\frac{a}{4}\right). \end{aligned} \quad (2.41)$$

The displacement we consider is the one which lifts the degeneracy of the  $|\Gamma_3^\pm\rangle$  doublet (as determined from the X-ray diffraction measurement [52] and the group theoretical arguments [4]):

$$(\beta, \beta, -2\beta), (\beta, \beta, 2\beta), (\beta, -\beta, -2\beta), (-\beta, \beta, -2\beta), \\ (\beta, -\beta, 2\beta), (-\beta, -\beta, -2\beta), (-\beta, \beta, 2\beta), (-\beta, -\beta, 2\beta).$$

The shorthand notation  $(-\beta, -\beta, 2\beta)$  is used to describe these displacements. The final positions of T metal ions following this displacement are:

$$\left(\frac{a}{4} + \beta, \frac{a}{4} + \beta, \frac{a}{4} - 2\beta\right), \left(\frac{a}{4} + \beta, \frac{a}{4} + \beta, -\frac{a}{4} + 2\beta\right), \left(\frac{a}{4} + \beta, -\frac{a}{4} - \beta, \frac{a}{4} - 2\beta\right), \\ \left(-\frac{a}{4} - \beta, \frac{a}{4} + \beta, \frac{a}{4} - 2\beta\right), \left(\frac{a}{4} + \beta, -\frac{a}{4} - \beta, -\frac{a}{4} + 2\beta\right), \left(-\frac{a}{4} - \beta, -\frac{a}{4} - \beta, \frac{a}{4} - 2\beta\right), \\ \left(-\frac{a}{4} - \beta, \frac{a}{4} + \beta, -\frac{a}{4} + 2\beta\right), \left(-\frac{a}{4} - \beta, -\frac{a}{4} - \beta, -\frac{a}{4} + 2\beta\right).$$

By using Eq. 1.11, and the difference between the final and initial positions of T metal ions calculated above, the total charge density  $\rho(\vec{r})$  pertinent to the displaced T metal ions can be calculated:

$$\rho(\vec{r}) = 2e \left[ \delta\left(x - \frac{a}{4} - \beta\right)\delta\left(y - \frac{a}{4} - \beta\right)\delta\left(z - \frac{a}{4} + 2\beta\right) + \delta\left(x - \frac{a}{4} - \beta\right)\delta\left(y - \frac{a}{4} - \beta\right) \right. \\ \delta\left(z + \frac{a}{4} - 2\beta\right) + \delta\left(x - \frac{a}{4} - \beta\right)\delta\left(y + \frac{a}{4} + \beta\right)\delta\left(z - \frac{a}{4} + 2\beta\right) + \delta\left(x + \frac{a}{4} + \beta\right) \\ \delta\left(y - \frac{a}{4} - \beta\right)\delta\left(z - \frac{a}{4} + 2\beta\right) + \delta\left(x - \frac{a}{4} - \beta\right)\delta\left(y + \frac{a}{4} + \beta\right)\delta\left(z + \frac{a}{4} - 2\beta\right) \\ \left. + \delta\left(x + \frac{a}{4} + \beta\right)\delta\left(y + \frac{a}{4} + \beta\right)\delta\left(z - \frac{a}{4} + 2\beta\right) + \delta\left(x + \frac{a}{4} + \beta\right)\delta\left(y - \frac{a}{4} - \beta\right) \right. \\ \left. \delta\left(z + \frac{a}{4} + 2\beta\right) + \delta\left(x + \frac{a}{4} + \beta\right)\delta\left(y + \frac{a}{4} + \beta\right)\delta\left(z + \frac{a}{4} - 2\beta\right) \right], \quad (2.42)$$

where  $2e$  is the charge carried by a single metal ion.

The quadrupole moment along the  $z$ -axis,  $Q_{33}$ , can be calculated by using the charge density from Eq. 2.42 in the Cartesian coordinate system:

$$Q_{33} = \int (3z^2 - r^2)\rho(\vec{r})d^3r$$

$$\begin{aligned}
&= \int (2z^2 - x^2 - y^2)\rho(\vec{r})dxdydz \\
&= 16e \left[ 2\left(\frac{a}{4} - 2\beta\right)^2 - 2\left(\frac{a}{4} + \beta\right)^2 \right] \\
&= -48ae\beta + 96e\beta^2 \\
&\approx -48ae\beta,
\end{aligned} \tag{2.43}$$

where  $\beta^2 \ll a^2$  since we use  $\beta \approx 10^{-4}a$  as suggested by Iwasa et al.[52] from X-ray diffraction measurements, the term containing  $\beta^2$  is neglected. Similarly,  $Q_{22} = 24ae\beta$ ,  $Q_{11} = 24ae\beta$ , and  $Q_{12} = Q_{13} = Q_{23} = 0$ , indicates that the quadrupole moment possessed by the T metal ions, displaced in a unique direction  $(\beta, \beta, -2\beta)$ , resembles a linear quadrupole form. If the displacement direction is reversed,  $Q_{33}$  changes sign. Other possible displacement directions for the T metal ions which resembles a linear quadrupole form with other orientations are  $(\beta, -2\beta, \beta)$  and  $(-2\beta, \beta, \beta)$ . Note that the initial configuration Eq. 2.41 possesses no quadrupole moment. The monopole and dipole moments of the difference between undisplaced (initial) and displaced configurations,  $\rho_{diff}(\vec{r}) = \rho(\vec{r}) - \rho_{initial}(\vec{r})$ , vanish.

Substituting  $\beta \approx 10^{-4}a$  and using an average value of  $a \approx 8\text{\AA}$  for praseodymium-filled skutterudites in Eq. 2.43, an approximate value for  $Q_{33}$  is obtained:

$$Q_{33} \approx -5 \times 10^{-40} \text{m}^2\text{C} \tag{2.44}$$

which is approximately 20 times higher than the quadrupole moment  $Q_{33}$  of the Pr  $4f^2$  electrons in state  $|\Gamma_3^\pm\rangle$  as mentioned in Eq. 2.37. More precise values for three different compounds are given in Table 2.1.

Table 2.1: The lattice constants and quadrupole moments possessed by the T metal ions due to  $(\beta, \beta, -2\beta)$  displacement from their initial positions where  $\beta \approx 10^{-4}a$ .

Skutterudites	$a$ (Å)	$Q_{33}$ ( $10^{-40}\text{m}^2\text{C}$ )
PrFe <sub>4</sub> P <sub>12</sub>	7.83	-4.7
PrOs <sub>4</sub> Sb <sub>12</sub>	9.30	-6.6
PrRu <sub>4</sub> P <sub>12</sub>	8.05	-5.0

## 2.7 The long-range quadrupole-quadrupole interaction energies $U_{quad}$ between the Pr $4f^2$ electrons and T metal ions

Due to the periodicity of the lattice, one can express the distances between the centers of the two quadrupoles considered in the previous section as:

$$d = Na,$$

where  $N$  is the number of unit cells and  $a$  is the lattice constant of the filled skutterudite. Replacing  $d$  by  $Na$  in Eqs. 1.22, 1.23 and 1.24 further simplifies the quadrupole interaction formula.

For case I:

$$U_{quad}^I = \frac{1}{4\pi\epsilon_0} \left( \frac{3Q_{33}Q'_{33}}{2N^5a^5} \right). \quad (2.45)$$

For case II:

$$U_{quad}^{II} = \frac{1}{4\pi\epsilon_0} \left( \frac{9Q_{33}Q'_{33}}{16N^5a^5} \right). \quad (2.46)$$

For case III:

$$U_{quad}^{III} = -\frac{1}{4\pi\epsilon_0} \left( \frac{3Q_{33}Q'_{22}}{4N^5a^5} \right). \quad (2.47)$$

Table 2.2: The long-range Pr-Pr quadrupole interaction energies between the Pr  $4f^2$  electrons in states  $|\Gamma_3^+\rangle$  and  $|\Gamma_3^-\rangle$  where  $\mathcal{A}$  has units of  $\text{m}^2$ .

Cases	$U_{quad}^{Pr-Pr} (10^{34} N^{-5} \mathcal{A}^2 \text{ eV/m}^4)$		
	PrFe <sub>4</sub> P <sub>12</sub>	PrOs <sub>4</sub> Sb <sub>12</sub>	PrRu <sub>4</sub> P <sub>12</sub>
I	-20.7	-8.8	-18.1
II	-7.8	-3.3	-6.8
III	10.4	4.4	9.0

The quadrupole moments  $Q$  and  $Q'$  may each be associated with either the quadrupole moment possessed by the crystal field ground state of the Pr  $4f^2$  electrons or the quadrupole moment due to the unique displacement of the T metal ions.

Using the quadrupole interaction energy formulas Eqs. 2.45, 2.46, and 2.47, and the calculated values of the quadrupole moments of the Pr  $4f^2$  electrons (Eqs. 2.36 and 2.40) and of T ion displacements in Table 2.1, the long-range quadrupole-quadrupole interaction energy can be calculated for three different cases: i) Pr-Pr which is the quadrupole interactions between two Pr ions, ii) Pr-T which is the quadrupole interactions between a Pr ion and a uniquely displaced T metal ion, and iii) T-T which is the quadrupole interaction between the two sets of uniquely displaced T metal ions. These results are tabulated in Tables 2.2, 2.3 and 2.4 respectively for three different relative orientations of the quadrupoles (cases I, II and III discussed in Section 1.11).

## 2.8 Interpretation

From Eqs. 2.37 and 2.44, the quadrupole moment due to the T ion displacement is approximately 20 times higher than the quadrupole moment of the Pr  $4f^2$  electrons

Table 2.3: The long-range T-T (Fe-Fe, Os-Os, Ru-Ru) quadrupole interaction energies between the T metal ions displaced in directions  $(\beta, \beta, -2\beta)$  and  $(-\beta, -\beta, 2\beta)$  where  $\beta$  has units of m.

Cases	$U_{quad}^{T-T}$ ( $10^{21}N^{-5}\beta^2$ eV/m <sup>2</sup> )		
	PrFe <sub>4</sub> P <sub>12</sub>	PrOs <sub>4</sub> Sb <sub>12</sub>	PrRu <sub>4</sub> P <sub>12</sub>
I	-10.4	-6.2	-9.6
II	-3.9	-2.3	-3.6
III	5.2	3.1	4.8

Table 2.4: The long-range Pr-T (Pr-Fe, Pr-Os, Pr-Ru) quadrupole interaction energies between the Pr 4f<sup>2</sup> electrons in state  $|\Gamma_3^{\mp}\rangle$  and T metal ions displaced in the directions  $(\pm\beta, \pm\beta, \mp 2\beta)$  where  $\mathcal{A}$  has the units of m<sup>2</sup> and  $\beta$  has units of m.

Cases	$U_{quad}^{Pr-T}$ ( $10^{28}N^{-5}\mathcal{A}\beta$ eV/m <sup>3</sup> )		
	PrFe <sub>4</sub> P <sub>12</sub>	PrOs <sub>4</sub> Sb <sub>12</sub>	PrRu <sub>4</sub> P <sub>12</sub>
I	4.6	2.4	4.2
II	1.8	0.9	1.6
III	-2.3	-1.2	-2.1

Table 2.5: Comparison of quadrupole-quadrupole interaction energies in  $\text{PrFe}_4\text{P}_{12}$  for  $N = 1$ .

Cases	$U_{quad}$ ( $10^{-7}\text{eV}$ )		
	Pr-Pr	T-T	Pr-T
I	-1.9	-637.6	34.6
II	-0.7	-239.1	13.0
III	1.0	318.8	-17.3

Table 2.6: Comparison of quadrupole-quadrupole interaction energies in  $\text{PrFe}_4\text{P}_{12}$  for  $N = 2$ .

Cases	$U_{quad}$ ( $10^{-9}\text{eV}$ )		
	Pr-Pr	T-T	Pr-T
I	-5.9	-1993.0	108.0
II	-2.2	-747.4	40.5
III	3.0	996.5	-54.0

in the states  $|\Gamma_3^\pm\rangle$ .

In order to calculate the Pr-Pr, T-T and Pr-T quadrupole-quadrupole interaction energies for  $N = 1$  ( $d = a$ ) and  $N = 2$  ( $d = 2a$ ) in  $\text{PrFe}_4\text{P}_{12}$ ,  $\mathcal{A} \approx 9.6 \times 10^{-22}\text{m}^2$  (Eq. 2.11), and  $\beta \approx 10^{-4}a$  [52] are substituted in  $U_{quad}$  in Tables 2.2, 2.3 and 2.4 respectively. The results are shown in Tables 2.5 and 2.6. The  $U_{quad}$  calculation follows the same pattern in cases of  $\text{PrOs}_4\text{P}_{12}$  and  $\text{PrRu}_4\text{P}_{12}$ .

The  $U_{quad}^{T-T}$  is found to be dominant quadrupole interactions in the filled skutterudites. One can make arbitrary choices of  $N$ . All three quadrupole-quadrupole interaction energies ( $U_{quad}^{Pr-Pr}$ ,  $U_{quad}^{T-T}$  and  $U_{quad}^{Pr-T}$ ) are the largest in  $\text{PrFe}_4\text{P}_{12}$ , and the least in  $\text{PrOs}_4\text{Sb}_{12}$  because of their different lattice constants.

Although the quadrupole moment of the T displacements  $Q_{33}^T$  was found to be approximately 20 times larger than the Pr  $4f^2$  electron quadrupole moment  $Q_{33}^{Pr}$ , these may still be considered to be relatively close given the sensitivity of  $Q_{33}^T$  to the parameter  $\beta$ , and the approximation used in obtaining  $\mathcal{A}$ . Therefore both types of quadrupoles, hence all these types of quadrupole-quadrupole interactions, are expected to be relevant to the various phenomena associated with quadrupole interactions in the praseodymium-filled skutterudites.



## Chapter 3

# Discussion and Summary

### 3.1 Discussion

The present work is based on a number of assumptions that raise several issues regarding this research. In this section, a number of these issues, along with their implications for continuing this research, will be discussed.

Firstly, the present study assumes that the Pr  $4f^2$  electrons are either in  $|\Gamma_3^+\rangle$  or in  $|\Gamma_3^-\rangle$  state, which may or may not necessarily be true. If a linear combination of these states of the type  $\alpha_1 |\Gamma_3^-\rangle + \alpha_2 |\Gamma_3^+\rangle$  is taken as the ground state for these electrons, the combination would clearly accommodate the  $4f^2$  electrons, and the calculations would more accurately reflect the real situation. There would be greater accuracy on the charge density calculation and, in turn, of the quadrupole moment possessed by the Pr  $4f^2$  electrons. The quadrupole moment resulting from the linear combination of two eigenstates of the doublet may either resemble a linear quadrupole form or a square quadrupole form.

Secondly, there is a crude approximation made of the radial part  $\mathcal{A}$  of the Pr  $4f^2$  electron distribution. According to this approximation, as taken from [50], the Pr

$4f^2$  electrons are confined within a radius ( $R_0$ ) which is equivalent to the maximum orbital radius of  $\text{Pr}^{3+}$  ions. An effort should be made to find the accurate radial part  $\mathcal{A}$  for the itinerant  $4f^2$  electrons so that an actual number density of charges can be calculated and, in turn, the quadrupole moment.

Thirdly, to better describe the quadrupole interaction mechanism, it is essential to explain the short-range interaction as well, which the present study lacks. This is because the short-range interaction is of greater magnitude than the long-range interaction. Although the former interaction is more important than the latter, the author is interested in comparing the long-range quadrupole interactions for three specific alignments of Pr-Pr, Pr-T and T-T in the present work.

Fourthly, long-range quadrupole interaction energies for three specific alignments of the Pr-Pr, Pr-T and T-T are calculated in Chapter 2. The T-T interaction is the highest, the Pr-Pr is the lowest whereas the Pr-T interaction energy is moderate. Although the T-T interaction is the dominant quadrupole interactions in the filled skutterudites, the Pr-Pr and the Pr-T interactions should not be ignored in the overall quadrupole interaction.

Fifthly, the present work is based on the assumption that the screening effect of the conduction electrons are neglected. In fact, the screening effect of the conduction electrons reduces the size of the quadrupole interactions.  $\text{PrFe}_4\text{P}_{12}$  and  $\text{PrOs}_4\text{Sb}_{12}$  are metals at low temperature, and therefore have conduction electrons. The screening effect applies to these skutterudites, and a reduced quadrupole interaction energy is expected. However,  $\text{PrRu}_4\text{P}_{12}$  is a non-metal at low temperature, and therefore has no conduction electrons, so that no screening effect applies. For this reason, the quadrupole interaction energy calculated for  $\text{PrRu}_4\text{P}_{12}$  will be more accurate as compared to the interaction energies for  $\text{PrFe}_4\text{P}_{12}$  and  $\text{PrOs}_4\text{Sb}_{12}$ .

Sixthly, it was speculated that the quadrupole interactions between the Pr  $4f^2$

electrons and the charges of the conduction electrons is the cause of heavy fermion superconductivity in  $\text{PrOs}_4\text{Sb}_{12}$ , and for the heavy fermion behavior evident in all of the praseodymium-filled skutterudites considered in the present study [1]. The quadrupole moment of the conduction electrons should be calculated to determine the interaction energy, which the present study lacks.

Seventhly, the displacements of pnictogens (X) is tantamount to a quadrupole moment. The quadrupole moment due to the displacements of pnictogens are ignored in the present study. In order to develop a microscopic theory of quadrupole interactions in the praseodymium-filled skutterudites, quadrupole interactions of pnictogens with rare earth ions, transition ions displacements and conduction electrons should be taken into account.

Lastly, this study is a first step toward developing a dynamical theory of quadrupole interactions in praseodymium-filled skutterudites. The complete Hamiltonian of the dynamical theory of quadrupole interaction should include short- and long-range quadrupole interaction terms and self-energy terms, and should look as follows:

$$H = H_{lr} + H_{sr} + H_{c-q} + H_c, \quad (3.1)$$

where  $H_{lr}$  is the Hamiltonian of long-range interactions among the Pr  $4f^2$  electrons and T metal ions, and  $H_{sr}$  is the Hamiltonian of the short-range interactions between them.  $H_{c-q}$  is the Hamiltonian of interactions between the charges of the conduction electrons and the quadrupole moment due to the Pr  $4f^2$  electrons, and  $H_c$  is the Hamiltonian of the conduction electrons.

## 3.2 Summary

This thesis represents the first step in the development of a theory of quadrupole interactions in the Pr-filled skutterudites. The main results are analytic calculations of the quadrupole moment carried by Pr  $4f^2$  electrons and transition ion displacements and their resulting interaction energies.

The quadrupole moments of the Pr  $4f^2$  electron ground states  $|\Gamma_3^\pm\rangle$  are calculated to be  $\pm 0.168080811e\mathcal{A}$ , where  $e$  is the charge of the positron, and  $\mathcal{A}$  is a quantity with units of  $\text{length}^2$  that depends on the radial distribution of charge of the  $4f^2$  electrons. This is found to be approximately  $9.6 \times 10^{-22}\text{m}^2$ , yielding a quadrupole moment of the order of  $\pm 2.6 \times 10^{-41}\text{m}^2\text{C}$ .

The quadrupole moment of the transition ion displacements in the direction  $(\pm\beta, \pm\beta, \mp 2\beta)$  is found to be  $\approx \mp 48ae\beta$ , where  $\beta$  is the size of the displacement. Using  $\beta \approx 10^{-4}a$ , the quadrupole moment carried by the transition ions displacements is found to be approximately  $\mp 5 \times 10^{-40}\text{m}^2\text{C}$ .

With these various approximations, the quadrupole moment carried by the transition ion displacements is found to be approximately twenty times larger than that of the Pr  $4f^2$  electrons. This difference is reflected in the relative sizes of the quadrupole interaction energies, for the three cases studied in this thesis: Pr-Pr, Pr-T and T-T interactions.

The next step in the development of a theory of quadrupole interactions would be the calculation of short range interaction energies. In particular, the interaction energy associated with a  $\text{Pr}^{3+}$  ion and the nearest transition ions must be considered. Such a theory could describe quadrupole ordering of Pr ions and structural transitions associated with transition ion displacements. However, in order to account for heavy fermion behaviour and heavy fermion superconductivity, the theory must be extended

to include quadrupole interactions with conduction electrons.

# Appendix A

## Appendix

### A.1 Electric field gradient due to a quadrupole

Using Eqs. 1.17 and 1.18, the quadrupole field can be expressed in the form as follows:

$$\begin{aligned}
 4\pi\epsilon_0 E_{quad}^j(\vec{r}) &= -\frac{\partial}{\partial r_j} \frac{r_l Q_{lm} r_m}{2r^5} \\
 &= -\frac{1}{2r^5} \left( \delta_{lj} Q_{lm} r_m + r_l Q_{lm} \delta_{mj} \right) - \frac{r_l Q_{lm} r_m}{2} \frac{\partial}{\partial r_j} r^{-5} \\
 &= -\frac{1}{2r^5} \left( Q_{mj} r_m + r_l Q_{lj} \right) + \frac{5}{2r^7} r_j r_l Q_{lm} r_m \\
 &= \frac{5}{2r^7} r_j r_l Q_{lm} r_m - \frac{1}{2r^5} \left( r_l Q_{lj} + Q_{jm} r_m \right) \tag{A.1}
 \end{aligned}$$

The field gradient can be written as:

$$\begin{aligned}
 4\pi\epsilon_0 \frac{\partial E_{quad}^j}{\partial r_i} &= \frac{\partial}{\partial r_i} \left( \frac{5}{2r^7} r_j r_l Q_{lm} r_m - \frac{1}{2r^5} (r_l Q_{lj} + Q_{jm} r_m) \right) \\
 &= \frac{1}{2r^7} \left( 5\delta_{ij} r_l Q_{lm} r_m + 5r_j \frac{\partial}{\partial r_i} (r_l Q_{lm} r_m) \right) \\
 &\quad - \frac{2}{\partial r_i} (r^2 r_l Q_{jl}) - \frac{7r_i}{2r^9} \left( 5r_j r_l Q_{lm} r_m - 2r^2 r_l Q_{lj} \right) \\
 &= -\frac{35}{2r^9} r_i r_j r_l Q_{lm} r_m + \frac{1}{2r^7} \left( 10r_i Q_{jl} r_l + 10r_j Q_{il} r_l \right. \\
 &\quad \left. + \delta_{ij} r_l Q_{lm} r_m \right) - \frac{1}{r^5} Q_{ij} \tag{A.2}
 \end{aligned}$$

## A.2 Spherical Harmonics

Listed below are the spherical harmonics for  $l = 3$  and all possible orientations of  $l$  [42, 44].

$$\begin{aligned}
 Y_3^0(\theta, \phi) &= \sqrt{\frac{7}{4\pi}} \left( \frac{5 \cos^3 \theta}{2} - \frac{3 \cos \theta}{2} \right) \\
 Y_3^1(\theta, \phi) &= -\sqrt{\frac{21}{64\pi}} \sin \theta (5 \cos^2 \theta - 1) \exp(i\phi) \\
 Y_3^{-1}(\theta, \phi) &= \sqrt{\frac{21}{64\pi}} \sin \theta (5 \cos^2 \theta - 1) \exp(-i\phi) \\
 Y_3^2(\theta, \phi) &= \sqrt{\frac{105}{32\pi}} \sin^2 \theta \cos \theta \exp(2i\phi) \\
 Y_3^{-2}(\theta, \phi) &= \sqrt{\frac{105}{32\pi}} \sin^2 \theta \cos \theta \exp(-2i\phi) \\
 Y_3^3(\theta, \phi) &= -\sqrt{\frac{35}{64\pi}} \sin^3 \theta \exp(3i\phi) \\
 Y_3^{-3}(\theta, \phi) &= \sqrt{\frac{35}{64\pi}} \sin^3 \theta \exp(-3i\phi)
 \end{aligned} \tag{A.3}$$

# Bibliography

- [1] E. D. Bauer, N. A. Frederick, P. -C. Ho, V. S. Zapf and M. B. Maple, *Phys. Rev. B* **65**, 100506, (2002).
- [2] M. B. Maple, P. -C. Ho, V. S. Zapf, N. A. Frederick, E. D. Bauer, W. M. Yuhasz, F. M. Woodward and J. W. Lynn, *J. Phys. Soc. Jpn.* **71**, 23, (2002).
- [3] M. S. Torikachvili, J. W. Chen, Y. Dalichaouch, R. P. Guertin, M. W. McElfresh, C. Rossel, M. B. Maple and G. P. Meissner, *Phys. Rev. B* **36**, 8660, (1987).
- [4] S. H. Curnoe, H. Harima, K. Takegahara and K. Ueda, *Phys. Rev. B* **70**, 245112, (2004).
- [5] S. H. Curnoe, H. Harima, K. Takegahara and K. Ueda, *Physica B* **312-313**, 837, (2002).
- [6] C. Sekine, T. Uchiumi, I. Shirotnani, and T. Yagi, *Phys. Rev. Lett* **79**, 3218, (1997).
- [7] D. Cao, R. H. Heffner, F. Bridges, I. -K. Jeong, E. D. Bauer, W. M. Yuhasz, and M. B. Maple, *Phys. Rev. Lett* **94**, 036403, (2005).
- [8] W. Jeitschko and D. J. Braun, *Acta Crystallography B***33**, 3401, (1977).

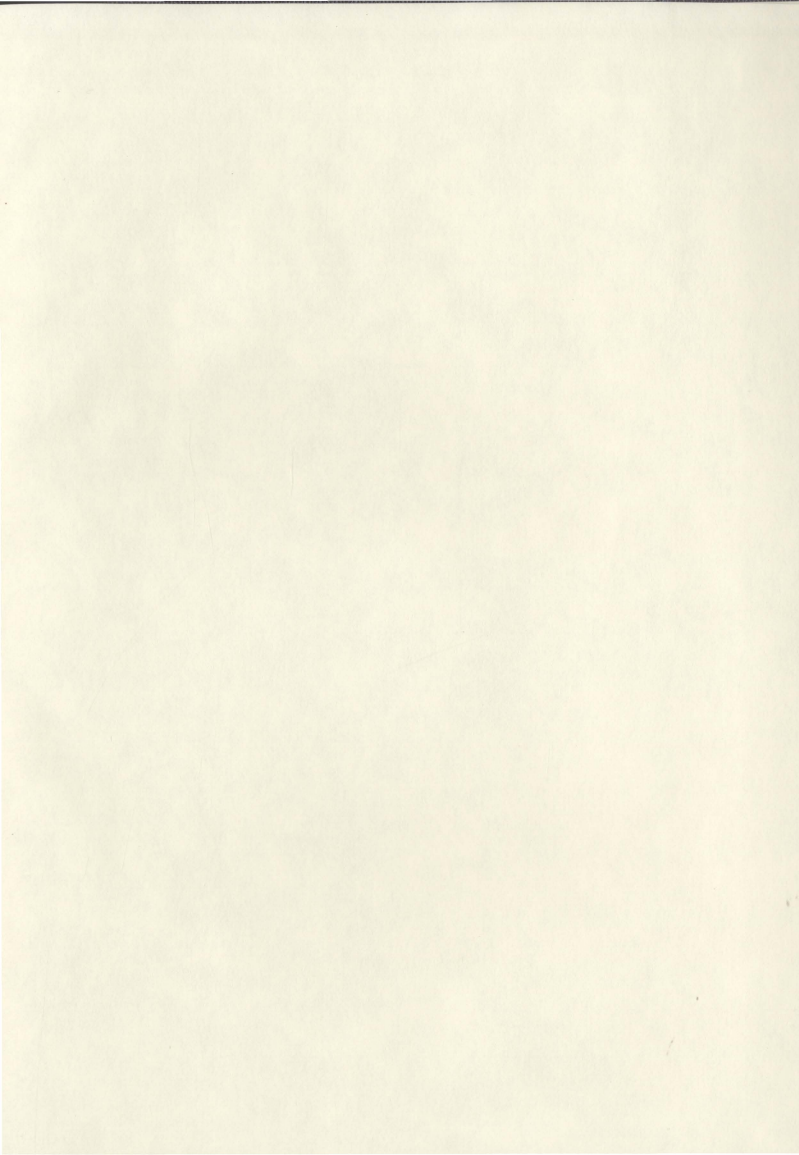


- [9] G. P. Meisner, M. S. Torikachvili, K. N. Yang, M. B. Maple and R. P. Guertin, *J. Appl. Phys.* **57**, 3073, (1985).
- [10] K. A. Gschneidner, *Handbook on the Physics and Chemistry of Rare Earths*, Elsevier Publications, (2003).
- [11] C. Uher, *Semiconductors and Semi-metals*, Academic Press, San Diego, (2001).
- [12] D. J. Braun and W. Jeitschko, *J. Less-Common Metals* **76**, 33, (1980).
- [13] D. J. Braun and W. Jeitschko, *J. Less-Common Metals* **72**, 147, (1980).
- [14] B. C. Sales, D. Mandrus and R. K. Williams, *Science* **272**, (1996).
- [15] C. H. Lee, H. Oyanagi, C. Sekine, I. Shirotnani and M. Ishii, *Phys. Rev. B* **60**, 13253, (1999).
- [16] G. P. Meisner, *Physica B* **108**, 763, (1981).
- [17] F. Grandjean, A. Gerard, D. J. Braun and W. Jeitschko, *J. Phys. Chem. Solids* **45**, 877, (1984).
- [18] Y. Aoki, T. Namiki, T. D. Masuda, K. Abe, H. Sugawara and H. Sato, *Phys. Rev. B* **65**, 06446, (2002).
- [19] T. Tayama, T. Sakakibara, H. Sugawara and H. Sato, *J. Phys. Soc. Jpn.* **72**, 1516, (2003).
- [20] Y. Nakanishi, T. Simiju, M. Yoshijawa, A. Matsuda, H. Sugawara and H. Sato, *Phys. Rev. B* **63**, 184429, (2001).
- [21] A. Kiss, and P. Fazekas, *J. Phys.: Condens. Matter* **15**, S2109, (2003).

- [22] E. A. Goremychkin, R. Osborn, E. D. Bauer, M. B. Maple, N. A. Frederick, W. M. Yuhasz, F. M. Woodward and J. W. Lynn, *cond-mat/0404519*, (2004).
- [23] L. Hao, K. Iwasa, M. Nakajima, D. Kawana, K. Kuwahara, M. Kohgi, H. Sugawara, T. D. Matsuda, Y. Aoki, and H. Sato, *J. Alloys and Compounds* **516**, 323, (2001).
- [24] L. Keller, P. Fischer, T. Herrmannsdörfer, A. Donni, H. Sugawara, T. D. Matsuda, K. Abe, Y. Aoki and H. Sato, *J. Alloys and Compounds* **516**, 323, (2001).
- [25] T. D. Matsuda, H. Okada, H. Sugawara, Y. Aoki, H. Sato, A. V. Andreev, Y. Shiokawa, V. Sechovsky, T. Honma, E. Yamamoto and Y. Onuki, *Physica B* **281-282**, 220, (2000).
- [26] H. Sato, Y. Abe, H. Okada, T. Matsuda, H. Sugawara and Y. Aoki, *Physica B* **281-282**, 306, (2000).
- [27] H. Sato, K. Abe, H. Okada, T. D. Masuda, K. Sugawara and Y. Aoki, *Phys. Rev. B* **62**, 15125, (2000).
- [28] Y. Aoki, T. Namiki, S. Ohsaki, S. R. Saha, H. Sugawara and H. Sato, *J. Phys. Soc. Jpn.* **71**, 2098, (2002).
- [29] H. Sugawara, T. D. Matsuda, K. Abe, Y. Aoki, H. Sato, S. Nojiri, Y. Inada, R. Sattai and Y. Onuki, *Phys. Rev. B* **66**, 134411, (2002).
- [30] H. Sugawara, T. D. Matsuda, K. Abe, Y. Aoki, H. Sato, S. Nojiri, Y. Inada, R. Sattai and Y. Onuki, *J. Magn. Magn. Mater.* **98**, 226, (2001).
- [31] C. Sekine, T. Inaba, I. Shirovani, M. Yokoyama, H. Amitsuka and T. Sakakibara, *Physica B* **281-282**, 303, (2000).

- [32] M. Matsumoto and M. Koga, J. Phys. Soc. Jpn. **73**, 1135, (2004).
- [33] I. A. Sergienko and S. H. Curnoe, Phys. Rev. B **70**, 144522, (2004).
- [34] D. L. Cox and A. Zawadowski, Exotic Kondo Effects in Metals, CRC Press, (1999).
- [35] A. Beiser, Concepts of Modern Physics, McGraw Hill, (1995).
- [36] P. M. Mathews and K. Venkatesan, A Text Book of Quantum Mechanics, McGraw Hill, (1991).
- [37] L. -P. Levy, Magnetism and Superconductivity, Springer, (2000).
- [38] G. Herzberg, Atomic Spectra and Atomic Structure, Dover, (1944).
- [39] H. Haken and H. C. Wolf, The Physics of Atoms and Quanta, Springer-Verlag, (1996).
- [40] B. S. Tsukerblat, Group Theory in Chemistry and Spectroscopy, Academic Press, (1994).
- [41] C. Cohen-Tannoudji, B. Diu and F. Loloé, Quantum Mechanics, McGraw Hill, (1977).
- [42] J. D. Jackson, Classical Electrodynamics, 3rd Ed., John Wiley and Sons, New York, (1998).
- [43] G. E. Owen, Introduction to Electromagnetic Theory, Allyn and Bacon, Boston, (1963).
- [44] F. Melia, Electrodynamics, University of Chicago Press, Chicago, (2001).

- [45] E. J. Konopinski, *Electromagnetic Fields and Relativistic Particles*, McGraw-Hill, New York, (1981).
- [46] A. Shadowitz, *The Electromagnetic Field*, McGraw - Hill, New York, (1975).
- [47] P. Lorrain, D. R. Corson and F. Lorrain, *Electromagnetic Fields and Waves*, Freeman, New York, (1988).
- [48] A. M. Portis, *Electromagnetic Fields: Sources and Media*, Wiley, New York, (1978).
- [49] J. D. McGervey, *Introduction to Modern Physics*, Academic Press, New York, (1971).
- [50] <http://bic.beckman.uiuc.edu/periodic1/Pr.html>, Web Elements site.
- [51] H. A. Bethe and R. W. Jackiw, *Intermediate Quantum Mechanics*, W. A. Benjamin Inc, (1968).
- [52] K. Iwasa, Y. Watanabe, K. Kuwahara, M. Kohgi, H. Sugawara, T. D. Matsuda, Y. Aoki and H. Sato, *Physica B* **312**, 834, (2002).



THE UNIVERSITY OF CHICAGO

PHYSICS DEPARTMENT

PHYS 440

STATISTICAL MECHANICS

LECTURE 1

PROBABILITY THEORY

1.1

1.2

1.3

